CHARACTERIZING DNA NANOTUBE NUCLEATION AT A VARIETY OF TEMPERATURES AND MONOMER CONCENTRATIONS

by

Seth Reinhart

A thesis submitted to the Johns Hopkins University in conformity with the requirements for the degree of Master of Science in Engineering

Baltimore, Maryland

April 2017

Abstract

Increasingly, nanotechnology synthesis uses biological macromolecules as engineering materials such as peptides, RNA, and DNA for use in sporting goods, ceramics, computer hardware, automotive lubricants, and cosmetics. Still, biological processes are more precise and elegant than our modern day engineering capabilities. Kinetic studies on tubulin formation often examine this structure through the lens of crystal nucleation and growth. Inspired by this biological supramolecular crystallization process, we examine a bottom-up synthesis of DNA nanotubes using tile monomers made of DNA. DAE-E tile monomers self-assemble at concentrations high enough to significantly decrease the energy barrier to nucleation. This system uses a DNA origami nanostructure called a seed to reduce the barrier to nucleation allowing DNA nanotubes to self-assemble at low tile monomer concentrations.

Currently, studies only examine seeded nanotube nucleation at specific temperatures and monomer concentrations, while little is known about the effect these conditions have when changed. Here, we present nucleation of seeded DNA tile nanotubes over a range of temperatures and DNA tile concentrations to reveal control limits to nanotube growth using a specific seed by examining this growth with fluorescence microscopy. These experiments show that at higher temperatures seeded nucleation requires larger concentrations of tiles and control limits shrink. Tile monomer dilution experiments demonstrate the kinetic stability of mature nanotubes at 20 °C showing nanotubes become unstable below 20 nM of tile monomers. Furthermore, variations in seed design give the seed different properties such as stopping nanotube growth. This

study illuminates conditions where we could gain more control over the system and shows some examples of how seed properties depend on design.

Advisor: Dr. Rebecca Schulman

Secondary Reader: Dr. Michael Bevan

Acknowledgments

I would like to first thank my thesis advisor, Dr. Rebecca Schulman. She has taught me a lot not just about the field but about how to be a better researcher. Thank you for the support and for generously allowing me to work in your lab during my undergraduate years into my masters. Thank you to all of my fellow lab mates who helped me throughout this project. I especially want to thank Deepak Agrawal and Abdul Mohammed for training me when I first started. I am lucky to have had both of you to guide me in my research.

Table of Contents

Introduction

Nanotechnology is becoming increasingly ubiquitous. Already we have found sweeping uses for nanomaterials such as sporting goods [1], ceramics [2], computer hardware [3] [4], and automotive lubricants [5]. As the need arises for technology on this scale with precise nanoscale resolution, bottom-up self-assembly processes become progressively more appealing. Actin networks [6] [7] [8] [9] [10] [11] and cellular microtubule growth [12] [13] [14] [15] [16] [17] provide biological inspiration for these types of processes, but outside of the cell, engineered applications are still in the beginning stages.

For self-assembly processes to be achievable, we need materials that hold the information for the desired process. DNA acts as our biological information storage, and the precise properties of its base pairing make DNA uniquely capable as an engineering material for self-assembly processes. DNA tiles with tight crossover junctions form 2D patterned grids with potential application as nanowires or templates [18] [19] [20]; DNA origami techniques fold into a large variety of programmable shapes [21] [22]; polyhedrons with DNA architecture selectively expand and contract based on environmental signals showing promise in drug-delivery systems [23] [24]; and DNA nanomachines walk along linear tracks or act as molecular tweezers [25] [26] [27] [28].

Still, we can achieve a higher degree of control over these self-assembly processes by better understanding their nucleation. Using 2D DNA tiles [29] [30] to form 3D structures called DNA nanotubes [31] shows potential for templated nanowire architectures, encapsulation of multiple cargos, and programmable self-healing materials.

Any of these potential applications requires spatiotemporal control over their growth. Nucleating nanostructures called seeds provide this control. Here, we attempt to isolate optimal conditions for seeded DNA nanotube nucleation and growth with our current system and reveal where we can improve.

DNA nanotubes grown with a DAE-E tile system

DNA nanotubes [31] are cylindrical structures formed from DNA tile monomers. We use a set of two DAE-E tile monomers [29] [30] called REd and SEd tiles (Figure 1a). A high concentration of tile monomers in buffer solution decreases the energy barrier to nucleation allowing a nucleation event to occur. A nanotube (Figure 1b) has a facet with a varying circumference of some number of tile widths [31]. Free tile monomers in solution (defined here as tiles that are not yet part of an existing nanotube) can attach to either side of this facet. Thus, nanotubes can grow in both directions in 1D.

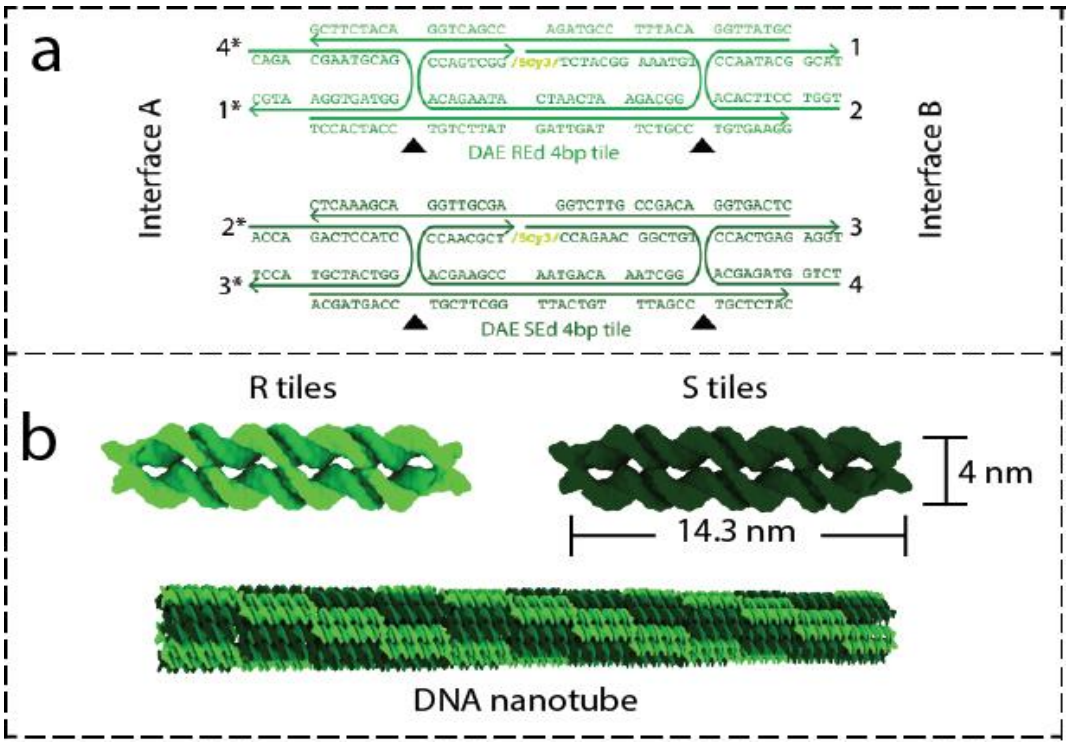

Figure 1: Schematic of (a) DNA tiles with their sequences and (b) tiles in a lattice structure cyclized into a nanotube.

At low concentrations of tiles the tile monomer equilibrium shifts such that nanotubes become unstable and all tiles are free in solution. The critical concentration of tile monomers is the lower limit at which mature nanotubes become unstable at a specific growth temperature thus the rate of tiles leaving the nanotube is the same as the rate of tiles sticking to the nanotube. The energy barrier to nucleation is greater than the energy barrier to growth [32], thus nucleated nanotubes will continue to grow even as tile monomers deplete in solution. The number of total nucleation events and the total length of all tubes in a system will increase until reaching an equilibrium between free tile monomers in solution and tile monomers in a nanotube. Diluting a system will decrease both the total length of nanotubes and number of nucleation sites until it again reaches equilibrium. Thus, at some low concentration, the critical concentration, even mature nanotubes become unstable leaving only free tile monomers in solution.

To lower the concentration of tile monomers needed to nucleate nanotube growth, a nanostructure called the RT (room temperature) A seed designed using DNA origami techniques [21] provides a template for tiles to attach. This nanostructure, called a seed, decreases the energy barrier for nucleation of DNA nanotubes [31] and thus allows nanotubes to grow at low tile concentrations. The seeds significantly reduce the amount of tiles needed to grow nanotubes and provides a deeper level of control over direction and placement of nanotube growth.

We want to reduce the energy barrier to nucleation and improve growth by changing the RT A seed but not the tiles, so we need to find those areas that a redesigned seed could improve upon. Together with our information on the critical concentration of nanotube stability, we can determine boundaries at which mostly seeded nucleation occurs. We have set the standard for acceptable percentage of seeded nanotubes (defined as nanotubes with a seed) in solution to be more than 50%. At conditions where the percentage falls below 50% an upper boundary exists past which we no longer desire to improve seeded nanotube nucleation with a seed redesign. With an upper boundary set by nanotube growth kinetics and a lower boundary set by nanotube stability, we have defined limits in which we wish to examine the nucleation efficiency of the RT A seed.

The conditions at which a seed redesign could possibly improve nanotube nucleation become apparent after defining boundaries set by nanotube stability and growth kinetics. Seeds lower the nucleation barrier for nanotube growth, but otherwise do not affect the thermodynamic and kinetic factors innate to the chemistry of the DNA tile monomers. Thus, a perfect seed would always nucleate a nanotube under any conditions that nanotubes are stable. Measurements of seed yield (defined as the percentage of seeds

nucleating a nanotube) empirically show the nucleation efficiency of the RT A seed at different conditions. With these measurements in mind, we can establish possible areas of improvement and examine seed redesigns within these parameters. A good seed redesign should improve upon nucleation efficiency by increasing seed yield where the seed yield of the RT A seed is low within our predefined boundaries.

After finding the conditions at which the RT A seed could improve, we desired to create designs that might be feasible options for a more perfect seed. First, we modified the sequences of the adapter complex sticky end strands. The RT A seed has two types of adapter complexes: REd and SEd [33]. The sequences for all the SEd adapter sticky end strands are identical, but the sequences for each of the three REd adapter sticky end strands differ (Appendix 5). Our original modification redesigns the adapter complexes such that the REd sticky end strands match in sequence (Appendix 7). We do not expect an improvement in nanotube nucleation for this modified RT A seed, but rather made the change to simplify our system. In hopes of improving the seed, we changed the sticky end strand in all the adapter complexes from DNA to RNA (Appendix 8). The sequences of the RNA sticky end strands are analogous to the sequences for the DNA sticky end strands, and otherwise all other adapter complex strands remain the same between the modified RT A seed and the RNA RT A seed. We expect an improvement in nucleation efficiency with this system because RNA binds to DNA more strongly than DNA binds to DNA [34]. This increase in affinity should lower the energy barrier barring nanotube nucleation.

We could also benefit from eliminating the excess scaffold strand not used in the seed. As the M13mp18 strand is 7,249 base pairs long [21] and the RT A seed only uses a third of these base pairs, the remaining ssDNA extends from the folded seed structure. This

excess can interfere with attachment of the seeds to specific sites or limit our ability to combine multiple seeds together at specific angles to each other. To avoid these problems, we could eliminate the excess ssDNA, but currently we use this excess as a site for dye attachment. A staple redesign (Appendix 15) allows us to attach the dye strands to the hairpins in the folded seed structure. We can now eliminate the excess ssDNA while retaining the ability to visualize our seed under a fluorescence optical microscope. An aPCR technique [35] cleaves the excess ssDNA leaving only the sequence needed for the DNA origami structure. This new structure, called the FLIP seed for Fluorescence Labelling In line with Pattern, effectively nucleates nanotube growth without excess single-stranded DNA on the scaffold.

A structure modified from the seed called a cap [33] provides further control over nanotube growth. The cap is analogous to the seed in design (Appendices 9-13). We designed the cap using DNA origami, and like the seed, it provides a template for nanotube nucleation. The template presented by the cap is complementary to the seed template and thus can attach to the growing end of seeded nanotubes. By measuring the lengths of seeded nanotubes before and after adding caps to solution we can show that caps stop nanotube growth.

Though we designed caps to stop nanotube growth, they can also nucleate nanotubes in solution. Redesigning the structure of the caps to create a floppier facet seems to reduce the ability of the cap to nucleate new nanotubes while retaining its ability to stop nanotube growth [33]. This new cap, called the flexible cap, stops nanotube growth without nucleating nanotubes.

Here, we show the control limits of the RT A seed and propose a possible redesign of the seed to improve on nucleation within these limits. We also show the FLIP seed design allows visualization of the seed making the unfolded portion of the scaffold strand unneeded. Caps provide a path to stopping nanotube growth with certain cap designs doing so without nucleating nanotubes. DNA nanostructures prove to be fruitful in gaining control of the DAE-E tile system.

Results and Discussion

In DNA nanotube self-assembling systems, seeds can reduce the nucleation barrier for growth. Our RT A seed works well to decrease the concentration of tile monomers necessary for tube growth in a buffer solution. Still, modifications to this seed design can increase its ability to nucleate and engage it in other capacities. For example, modifying the sequence of the sticky ends in the adapter complexes such that they are complementary to the growing ends of the nanotubes allows these structures to bind to the ends of the tubes and stop growth. Other modifications might further decrease the nucleation barrier for tile monomer self-assembly. Another redesign allows us to fluorescently visualize the seed without the extra single-stranded scaffold base pairs acting to sterically hinder the seed from attaching to specific sites. Here, we highlight the effect these modifications have on seed function. Furthermore, we characterize the RT A seed to show where changes in seed property are desired.

DAE-E DNA nanotubes grown at 20℃ become unstable at monomer concentrations lower than 20 nM.

At low concentrations of tile monomers, DNA nanotubes become thermodynamically unstable. For our DAE-E tile system (Appendix 1), we wanted to find the lower limit at which nanotubes became unstable and thus no seed could nucleate nanotube growth. We annealed tiles from 90 to 20℃ at a tile concentration of 100 nM. Nanotubes grow easily without the need for seeds to nucleate growth at this high tile monomer concentration. To allow the nanotubes time to fully grow and approach equilibrium we allowed the samples to sit in the thermocycler for 22 hours. At this point, 1x TAE buffer diluted these solutions to decrease the tile concentration in solution to 70,

50, 40, 30, 20, and 10 nM. The diluted solutions sat in the thermocycler for an additional 41 hours before imaging to again allow the nanotubes to approach a state of equilibrium. We imaged two samples for each dilution using fluorescence microscopy and observed nanotubes became unstable somewhere between 10 and 20 nM (Figure 2).

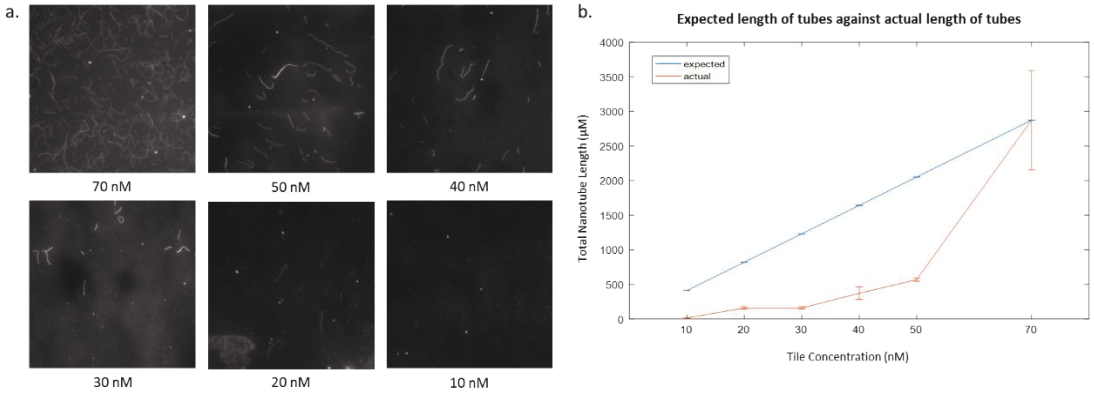

Figure 2: At 20℃, the equilibrium for nanotube formation shifts to favor unattached tile monomers in buffer solution between 10 and 20 nM. (a) Images of nanotubes grown at a monomer concentration of 100 nM at 20℃ diluted down to monomer concentrations of 70, 50, 40, 30, 20, and 10 nM. (b) The actual total length of nanotubes in solution is far less than the predicted total length of nanotubes based on the total length of nanotubes at 70 nM.

Though images of the nanotubes qualitatively show this dilution effect, we do not know if nanotube tiles are dissolving back into solution as free monomers or if the apparent effect is only a product of dilution. We measured the lengths of each nanotube in our image frames and found the total length of nanotubes for each dilution point. Based on the total length of nanotubes at 70 nM, we found the expected total length (or the total length of the nanotube we would predict based on 70 nM nanotube total length) of nanotubes at each lesser dilution by multiplying the total length at 70 nM by the ratio between the lesser concentration and 70 nM (x nM/70 nM). Data taken on the actual nanotube lengths at each dilution show the total length of nanotubes is far less than if tiles did not detach from

nanotubes. This disparity suggests that tiles became unstable as nanotubes and returned to solution as free tile monomers.

Increasing temperature reveals the need for an increase in tile monomer concentrations for nucleation.

After finding nanotubes become unstable below 20 nM, we characterized the RT A seed (Appendix 2). In these experiments, we looked at ranges of temperature and tile concentrations the RT A seed could efficiently nucleate nanotube growth and which areas could be improved upon. We define poor nucleation for conditions at which less than half of the seeds nucleate nanotubes and good nucleation for conditions at which more than 50% of seeds nucleate nanotubes. Furthermore, we set the conditions at which less than half of the nanotubes are seeded to be the upper boundary for possible areas of improvement by seed redesign alone. These arbitrary definitions allow us to characterize the quality of seeded nucleation for the RT A seed and compare the quality of seeded nucleation for any new seeds against this standard.

Our findings characterize the RT A seed under a variety of temperature and tile monomer conditions (Figure 3). We collected data at 20, 22, 24, and 26℃ at tile concentrations ranging from 15 nM to 500 nM. These data show that higher concentrations of tiles are needed for seeded nanotube nucleation at higher temperatures. For example, the point at which more than 50% of RT A seeds begin to nucleate nanotubes occurs at about 30 nM. In fact, by 45 nM the RT A seed begins to produce nucleation with about 71.1% of seeds nucleating nanotube growth. After 45 nM, we see only a modest increase in the percentage of seeds nucleating nanotubes.

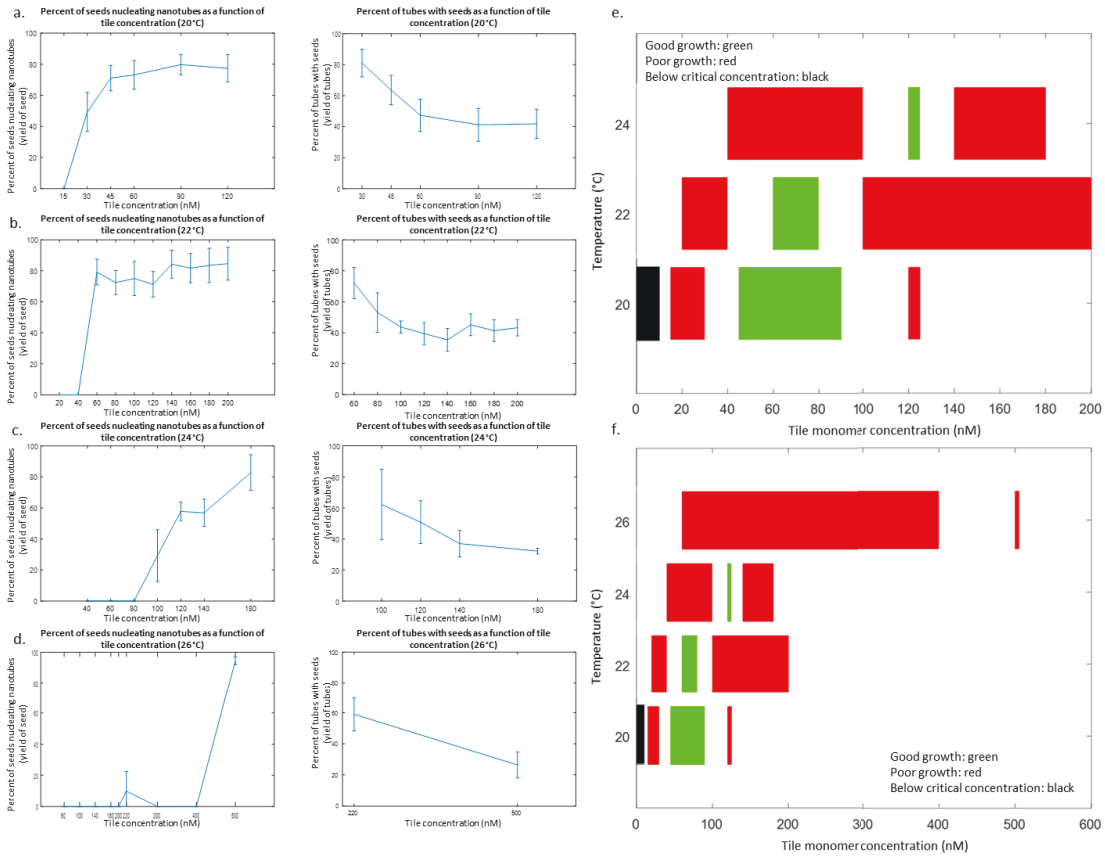

Figure 3: At higher temperatures, an increasing concentration of tile monomers are needed to obtain good nucleation and growth shown by graphs for seed yield and tube yield at (a) 20 °C, (b) 22 °C, (c) 24 °C, and (d) 26 °C. These data are collected in (e) for 20, 22, and 24 °C and (f) for 20, 22, 24, and 26 °C.

Raising the temperature by 2 degrees to 22℃ also raises the concentration of tile monomers needed for acceptable nanotube nucleation. We find poor nucleation up to 40 nM and good nucleation starts between 40 and 60 nM. At 60 nM, we see seed yields of about 80% with values for seed yield holding consistently at higher concentrations.

Further increasing the temperature to 24℃ presents a rapid increase in the number of tile monomers needed for good seeded nanotube nucleation. Poor nucleation persists until 100 nM with a steady rise into good nucleation by 120 nM of tiles. Finally, at 26℃ we observe little nanotube growth until 500 nM at which point the vast majority of RT A seeds are nucleating nanotubes.

With a steady rise in temperature, the amount of tile monomers needed for good nucleation rises rapidly. From 20 to 26℃, data show an increase in the necessary amount of tile monomers for good nucleation from 30-45 nM to 400-500 nM. This 10-fold increase suggests a rise in temperature hinders the ability of the RT A seed to nucleate nanotube growth.

Regions of good growth shrink as the temperature increases.

Our findings also suggest that the control limits of tile monomer concentrations diminish with increasing temperature (Figure 3). For example, at 20℃ good nucleation begins to occur between 30 and 45 nM. As monomer concentrations increase, it decreases the barrier to nucleation without a seed. For this reason, with more tiles in solution we consistently observe a rise in the number of unseeded nanotubes. The data show that the amount of unseeded nanotube growth becomes greater than 50% between 90 and 120 nM at 20℃. Thus, we have an upper limit for acceptable nanotube growth. At 20℃ our tile monomer concentrations can range from 30-45 nM to 90-120 nM, a 45-90 nM range.

At 22℃, we observe an acceptable amount of unseeded nanotube growth at 80 nM but an unacceptable amount by 100 nM. These data suggest an upper limit between 80 and 100 nM. Already at 22℃ the flexibility of tile monomer concentrations has diminished from 40-60 nM to 80-100 nM, a range of 20-60 nM. This flexibility decreases even further as we raise the temperature of nanotube growth to 24℃. At this temperature, we see too much unseeded growth at 140 nM shrinking our acceptable range from 100-120 nM to 120-140 nM. Good growth at 24℃ occurs in a small range of 0-40 nM of tile monomers. In fact, at 26℃ we never observe good nanotube growth since we do not observe growth at 400 nM and unseeded growth occurs too often at 500 nM. Still it should be noted that

experiments done on nanotube growth at 26℃ between 400 and 500 nM could reveal a range of concentrations in which good growth occurs.

The range of concentrations in which good growth occurs shrinks as the temperature rises. At 20℃ the range is 45-90 nM wide, then 40-60 nM at 22℃, and 20-60 nM at 24℃. The nucleation barrier rises with temperature more quickly than the energy barrier for tube growth causing the range of monomer concentrations at which the RT A seed works to effectively diminish. A seed that reduces the nucleation barrier more than the RT A seed might widen the range of good growth at each temperature point, but the ranges would still diminish as the temperature rises.

RNA seed shows potential to improve control over and reduce the nucleation barrier to tube growth.

One of the initial design changes to the RT A seed modified the adapter complexes. RNA binds to DNA with more affinity than DNA binds to DNA [34]. Thus, changing the sticky end strands of the adapter complexes from DNA to RNA might lower the nucleation barrier even further.

There are two types of adapter complexes in the RT A seed: REd and SEd [33]. These types are analogous to the two types of tiles used in the nanotubes. The sequence of the sticky end strands in the SEd adapter complexes are all the same, but this is not true for the sticky end strands in the REd adapter complexes (Appendix 5). Our first modification changes the REd adapter complexes so that sticky end strands have the same sequence (Appendix 7). This seed, referred to as the modified DNA RT A seed, still uses DNA for the sticky end strands. Now with only two strands (the REd and SEd adapter complex sticky end strands) rather than four to order as RNA, we make the final modification to the

original RT A seed. The sequences of the sticky end strands for the RNA RT A seed are the RNA equivalent of the sequences for the modified DNA RT A seed (Appendix 8).

We grew the RT A seed, modified DNA RT A seed, and RNA RT A seed at 20℃ with 45 nM of tiles. Images of nanotubes with each type of seed after 19, 28, 46, and 48 hours of growth show that the modified DNA RT A seed and RNA RT A seed nucleate nanotube growth. The RT A seed, modified DNA RT A seed, and RNA RT A seed nucleate nanotubes 56.1%, 54.5%, and 62% of the time respectively where these percentages are an average of the percentage of seeds nucleating nanotubes at each time point (Figure 4).

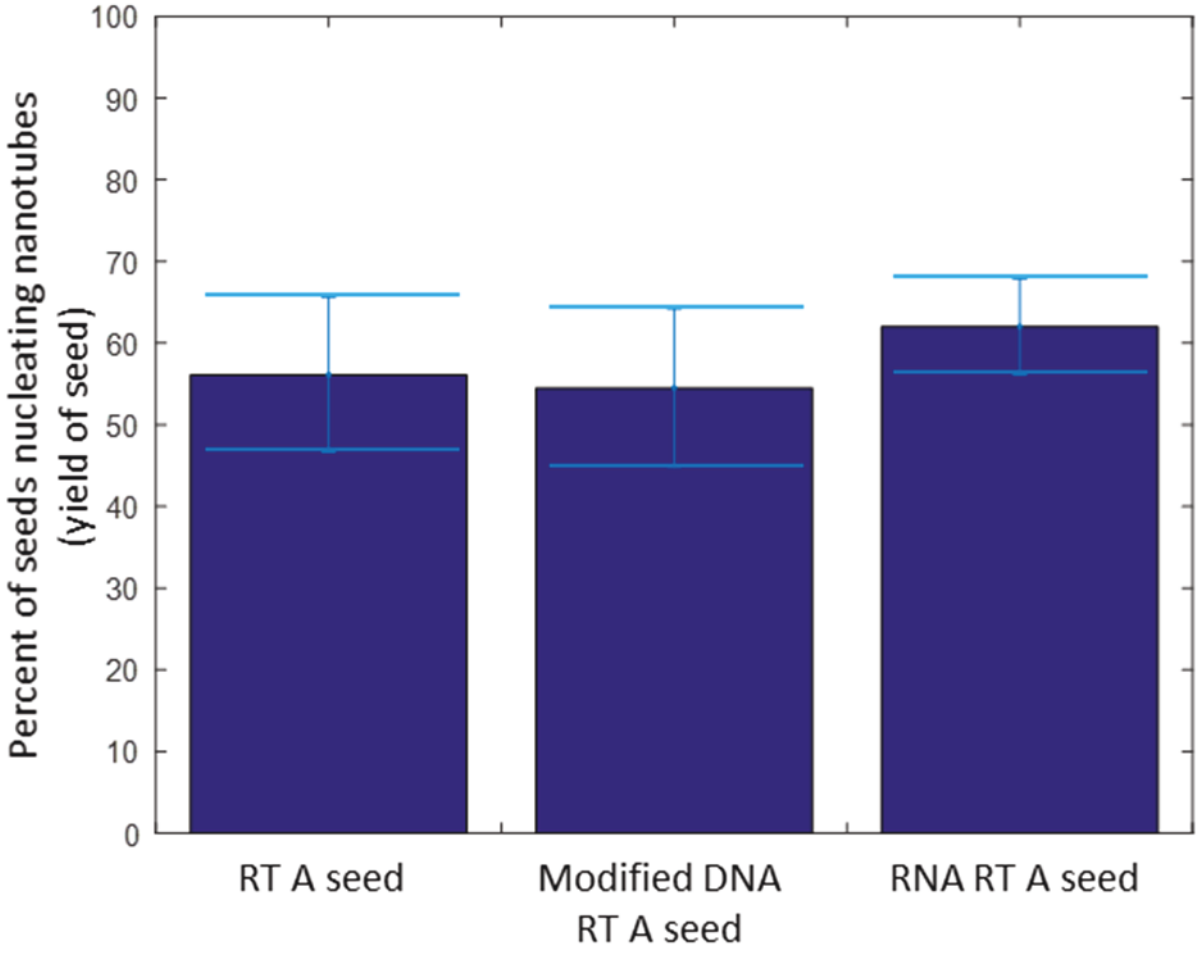

Figure 4: Percent of seeds nucleating nanotubes for each of the three types of seeds.

These data show the RNA RT A seed is moderately better than the original RT A seed at nucleating nanotube growth. It also shows that the modified DNA RT A seed nucleates growth approximately as well as the original RT A seed. We can expect these results since we predicted that RNA sticky end strands would nucleate more effectively than DNA sticky end strands. Though the sticky end strand sequences for the REd adapter complexes differ between the RT A seed and the modified DNA RT A seed the 4 nucleotides on each of the strands that act as the sticky ends are the same. Thus, a comparable amount of nucleation between these two seed types matches our expectations.

Future studies would compare the percentage of seeds nucleating nanotubes and the percentage of tubes with seeds for the modified DNA RT A seed and the RNA RT A seed against the data collected for the RT A seed in the previously mentioned characterization experiments. This comparison would elicit a deeper understanding of the effect our modifications on the RT A seed have had on the nucleation process. Preliminary data shows some promise for the RNA RT A seed.

New staple design allows fluorescence labels to attach to hairpins of seed.

In our seed designs, excess ssDNA not folded into the structure hangs from the scaffold strand. This excess ssDNA can sterically interfere with seed attachment onto a substrate or with the junction angle between two connected seeds. Fluorescent dyes attach to this excess in most of our seed designs to allow for optical visualization using fluorescence microscopy. Redesigning the staple pattern in the seed allows these dyes to attach to the hairpins rather than the excess ssDNA in the scaffold strand (Figure 5g).

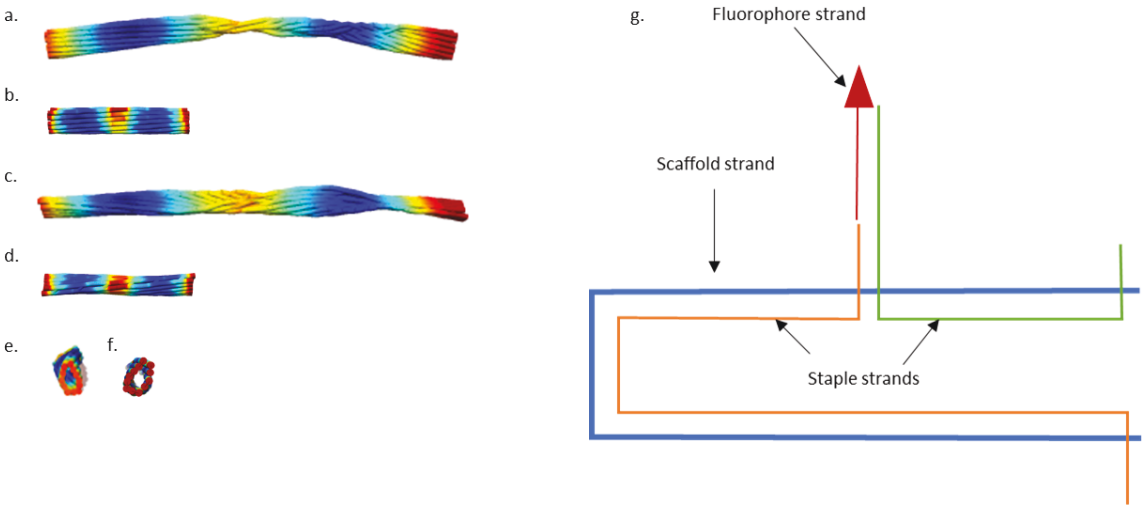

Figure 5: CanDo models of (b, d, and f) the original long seed *[31]* against (a, c, and e) the longer seed. Staples were redesigned for the FLIP seed (g).

Now that the excess ssDNA are no longer necessary for visualizing the structure, we must find a way to get rid of this part of the scaffold. With cadnano, we designed seeds extending the structure to use more scaffold, but CanDo models showed these structures would likely exhibit twisting and stress (Figure 5a-f). Instead, using aPCR [35], we cleaved off the unneeded DNA base pairs leaving only the scaffold necessary for the seed.

Caps can bind to ends of nanotubes and stop growth.

With the seed functioning to reduce the nucleation barrier to nanotube growth, it became apparent that an analogous structure could bind to the ends of the nanotubes. This structure would stop the growth of nanotubes by binding to the free end of nanotubes where free tile monomers could otherwise attach. Our design for the cap structure folds the scaffold M13mp18 strand with 24 staples (Appendix 10). These 24 staples fold a different part of the scaffold strand than folded by the 24 staples for the RT A seed [33]. The adapter complexes contain sticky end strands that are complementary to those used for the RT A seed as well as the tile sticky end strands at the growing end of the nanotube. We use atto488 to distinguish the cap from the seed which uses atto647. We call this capping structure with a full set of staples and adapters the rigid cap (Appendix 9 and 10).

The rigid cap stops growth of DNA nanotubes but can also nucleate nanotubes (Figure 6). To test the rigid caps ability to stop nanotube growth, we added 0.3 µl of caps to a solution with seeds that had been growing for 4 and 8 hours. In our control, we added buffer to similar seeded nanotube samples at the same volume as the caps. We imaged both samples with and without caps after 4.5, 8.5, 25, 32, and 50 hours. The mean length of nanotubes capped after 4 hours of growth was shorter than those nanotubes capped after 8 hours. In either case, the mean length of the nanotubes stopped growing and remained

consistent after adding the caps. In our control samples, nanotubes continued to grow and measurements show the mean length of nanotubes in these samples to be longer than capped nanotubes. This disparity between the mean length of nanotubes in samples with and without caps suggests that caps stop nanotube growth.

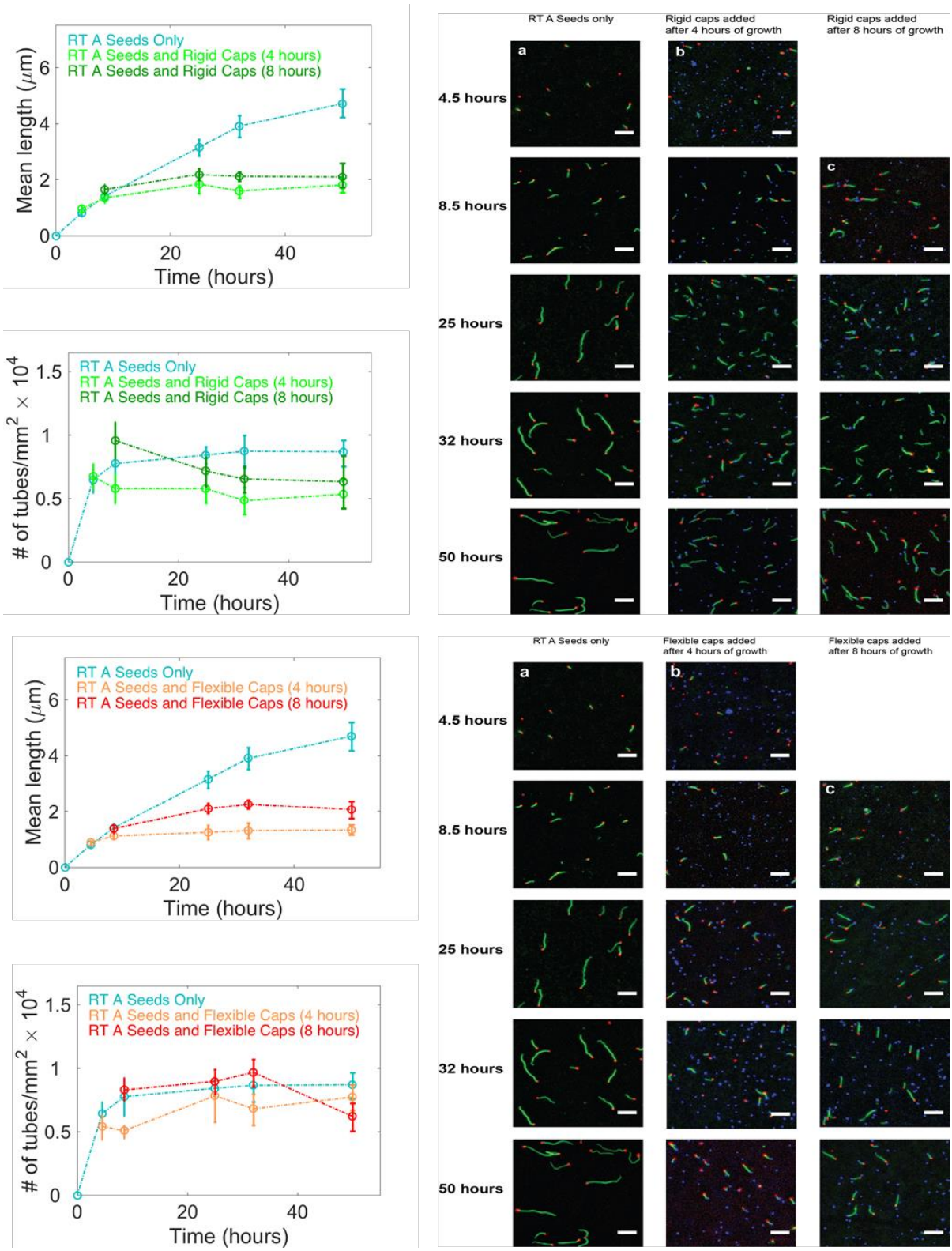

Figure 6: Graphs show the rigid cap and flexible cap stop growth. Optical images of nanotubes corroborate this finding.

Optical images of the nanotubes, RT A seeds, and rigid caps show many nanotubes with seeds on one end of the tube and caps on the other (Figure 6). These images provide evidence that caps stop growth by binding to the ends of nanotubes. Many of the tubes in these images have a cap on one end without a seed on the other. This combination suggests the rigid cap can nucleate tube growth.

We made a variety of adjustments to the cap design to find a cap that would retain its ability to stop growth but not its ability to nucleate. Removing staples from the rigid cap structure could cause the cap facet to become more flexible and removing adapters might create a facet less energetically favorable for nucleation. This flexibility would increase the energy barrier for nucleation eliminating the cap's ability to nucleate growth. It would also increase the energy barrier to capping, but we hoped not substantially. Less adapters in the facet of the cap would also increase the energy barrier for nucleation since a tile would rather bind to an adapter on both sides rather than just one [31]. Our designs removed the REd adapters in the rigid cap structure leaving only the SEd adapters.

After creating a library of caps each with a different modification (Appendix 11), we tested their ability to nucleate nanotube growth by putting 2 pM of each capping structure in a solution of annealed tiles for 25 hours. These experiments showed that a cap with no staples but a full set of adapters is least likely to nucleate growth. We call this cap the flexible cap and only about 1.2% of these structures nucleate growth in the absence of RT A seeds in a solution with a tile concentration of 45 nM. In time series experiments that measure the mean length of nanotubes in a solution after 4.5, 8.5, 25, 32, and 50 hours, the flexible cap stopped nanotube growth as effectively as the rigid cap.

By modifying the seed, we successfully altered its function to be able to stop nanotube growth rather than nucleate it. The rigid cap with a full set of adapter complexes and staples both nucleates and stops nanotube growth. The flexible cap retains its ability to stop nanotube growth but its lack of staples makes it unable to nucleate growth well.

Conclusion

We sought to understand and improve the RT A seed used to nucleate nanotubes for our DAE-E tile system. Here, we show that the RT A seed nucleates well at 20℃, but its performance quickly diminishes with increasing temperature. Though we cannot shift the control limits with a seed redesign, a better seed would nucleate nanotubes more often below 80 nM at 22℃, 120 nM at 24℃, and 400 nM at 26℃. An RNA seed might improve nucleation, but preliminary experiments suggest it would only do so marginally.

Furthermore, design changes to create the cap or the FLIP seed allow these DNA nanostructures to display control over the nanotubes in unique ways. The FLIP design makes the unfolded portion of the M13mp18 scaffold strand unnecessary and both the rigid and flexible cap successfully stop nanotube growth. These insights can provide valuable information in proceeding work on DNA nanotubes.

Materials & Methods

Experimental DNA nanotube structures

We characterized nucleation of DNA nanotubes with DAE-E tile monomers [29] and a specific nanostructure (or seed) folded using DNA origami [21]. Ten separate strands form a set of REd and SEd DAE-E DNA tiles with five strands for each tile (Appendix 1). We labelled the tiles with Cy3 fluorescent dye for imaging. To create the RT A seed, a set of 24 staple strands folded a section of M13mp18 single-stranded DNA used as a scaffold strand into a 3D cylindrical structure. We annealed the scaffold and staples together with an additional set of single-stranded dye attachment DNA, Atto 647N dye, and a set of 24 DNA strands used for the adapters (Appendices 14, 5, and 6).

The modified DNA RT A seed uses 4 individual adapter strands that are different from the RT A seed (Appendix 7). Since we modified the RT A seed to make the REd adapter complex sticky end strands the same, four strands from two adapter complexes needed different sequences. We left one REd adapter complex unchanged and used that sticky end strand for the other two REd adapter complexes. Only, the two strands on either side of the sticky end strand in the modified adapter complexes differ between the modified DNA RT A seed and the RT A seed. To create the RNA RT A seed, we simply changed the adapter sticky end strands in the modified DNA RT A seed from DNA to RNA (Appendix 8). Otherwise, the RNA RT A seed is the same as the modified DNA RT A seed.

Similarly, the rigid cap uses 24 staple strands to fold a portion of the scaffold strand not used by the RT A seed (Appendix 10). The scaffold and staples annealed with dye

attachment strands, Atto 488 dye, and a set of adapter strands (Appendices 14, 5, and 6). The adapter strands used for the cap are different than those used for the RT A seed. The sticky ends of the sticky end adapter strands for the cap are complementary to the sticky ends on the RT A seed. The flexible cap uses the same materials as the rigid cap except the flexible cap lacks staples. Both the rigid cap and the flexible undergo purification after annealing from 90 to 20℃.

The FLIP seed, adapted from a previously designed seed [31], uses a larger set of staples than the previously described structures. This seed uses a set of 72 staples [31] to fold either the full M13mp18 strands or a cleaved section of it. The atto647 dye strands attach to the staples at the hairpin turns. The adapter strands used by the FLIP seed are the same as those used by the RT A seed.

Seed and cap preparation

We annealed all seeds and caps separately from the tiles. Bayou Biolabs provided us with M13mp18 scaffold strands and Integrated DNA Technologies, Inc provided us with all other strands. IDT purified adapter sticky end strands with PAGE purification and fluorescently labelled strands with HPLC purification. We used all other strands directly after desalting. To prepare samples for purification we annealed both seeds and caps from 90 to 20℃. Samples contained 0.05 mg/ml of BSA biotin (A8549, Sigma-Aldrich Co.), 5 nM M13mp18 scaffold strand, 500 nM of each staple strand, 200 nM of each adapter complex sticky end strand, 100 nM of all other adapter complex strands, 25 nM of each dye attachment strand, and 5000 nM of dye strands. In all cases, annealing occurred in TAE Mg2+ buffer (a mixture of a 40 mM Tris-Acetate-1mM EDTA solution with a 12.5 mM magnesium acetate solution) from 90 to 20℃ in an Eppendorf Mastercycler.

Seed and cap purification protocol

After annealing 50 µl of seed or cap samples in an Eppendorf Mastercycler, we prepared the seeds or caps using a centrifugal purification process. In 100 kDa Amicon Ultra-0.5 ml Centrifugal Filter (UFC510096) tubes, we mixed the 50 µl sample with 350 µl of TAE Mg2+ buffer solution. This mixture centrifuged at 2000 RCF for 4 minutes. After this first wash, the samples centrifuged at the same settings 3 more times with an additional 200 µl of TAE Mg2+ buffer added to the filter between each wash. To obtain the purified seeds or caps from the filter, we inverted the filter into a clean tube and briefly centrifuged it until the liquid collected in the new tube. To obtain the concentration of purified seeds or caps, we imaged a not yet annealed 19.7 µl tile solution with 0.3 µl of seeds or caps using fluorescent microscopy.

Tile mix sample preparation

Tile solutions annealed from 90℃ and incubated at 20, 22, 24, or 26℃ in an Eppendorf Mastercycler in TAE Mg2+ buffer (a mixture of a 40 mM Tris-Acetate-1mM EDTA solution with a 12.5 mM magnesium acetate solution). Solutions contained 0.05 mg/ml of BSA biotin to keep tiles in bulk solution. This protein competes with other structures in the solution for space on the walls of the materials used in the experiments (PCR tubes, pipette tips, etc.) thus avoiding loss of tiles to these materials. Concentration of tile strands varied anywhere from 15 nM to 500 nM after addition of seeds and caps with sticky end strands present at double the concentration of the other tile strands. We ordered tile strands from Integrated DNA Technologies, Inc. IDT purified tile strands without fluorescent dyes using PAGE purification and with fluorescent dyes using HPLC purification. We added aliquots of 19.7 µl or 19.4 µl to the thermocyclers, thus each aliquot

contained tiles at slightly higher then intended concentrations during the annealing process. As the tile anneal reached its lowest temperature, 0.3 μl of purified seeds added to the annealed tile solution diluted the concentration of DNA tile monomers. Capping experiments allowed for the addition of 0.3 μl of caps some hours after the addition of seeds to allow time for the nanotubes to grow. In any case, the additional volumes added to the tile solutions diluted the samples to the intended concentration upon reaching 20 μl.

Fluorescent microscopy of the samples

We took images on an inverted microscope (Olympus IX71). To prepare the samples for imaging, we added 0.3 μl of 1.0 μM D01 strand, a 54 base pair sequence that does not interact with other DNA strands in the sample. D01 strand helps to visualize the nanotubes by competing with free tile monomers adsorbing to the slides. After adding this additional strand, we quickly pipetted 3 μl of sample (6 μl for capping experiments) onto a 18x18 mm cover slip and inverted that onto a glass slide. A 60X/1.45 NA oil immersion objective with a cooled CCD camera (iXon3, Andor) captured images of each sample. We captured 2 to 3 images of each sample. For each set of temperature and tile monomer concentration conditions examined for the RT A seed, we imaged three samples at a time, while we used only two samples for all other experiments.

Data Quantification technique

To measure the percentage of seeds nucleating nanotube growth and percentage of tubes with seeds, we counted the number of seeds, tubes with seeds, and tubes without seeds in each image. A MATLAB code flattened the coloring of the images with histogram equalization and overlaid multicolored images of seeds, tubes, and if present, caps. We

ignored tubes running off the edges of the image and tubes too entangled to track from end to end.

In some cases, we also needed to measure the lengths of each nanotube to find mean tube length and total tube length. By manually adjusting the brightness threshold for each tube image, we showed MATLAB where the nanotubes were allowing the program to convert the tubes into a binary form. Using MATLAB's bwmorph function, the program thinned the nanotubes into single-pixel curves. MATLAB calculated nanotube length by measuring the curve length in pixels and converting pixels to microns with the conversion of 0.017 microns for every 1 pixel.

Appendices

Appendix 1: REd and SEd tile sequences

REd tile sequences:

RE-4bp-1:	CGTATTGGACATTTCCGTAGACCGACTGGACATCTTCG
RE-4bp-2EE01:	TGGTCCTTCACACCAATACGGCAT
RE-4bp-3Cy3:	/Cy3/TCTACGGAAATGTGGCAGAATCAATCATAAGACACCAGTCGG
RE-4bp-4:	CAGACGAAGATGTGGTAGTGGAATGC
RE-4bp-5:	TCCACTACCTGTCTTATGATTGATTCTGCCTGTGAAGG

SEd tile sequences:

SE-4bp-1:	CTCAGTGGACAGCCGTTCTGGAGCGTTGGACGAAACTC
SE-4bp-2DIAG:	TCTGGTAGAGCACCACTGAGAGGT
SE-4bp-3Cy3:	/Cy3/CCAGAACGGCTGTGGCTAAACAGTAACCGAAGCACCAACGCT
SE-4bp-4DIAG:	ACCAGAGTTTCGTGGTCATCGTACCT
SE-4bp-5:	ACGATGACCTGCTTCGGTTACTGTTTAGCCTGCTCTAC

Here /Cy3/ denotes a covalently attached Cy3 fluorophore

Appendix 2: RT A seed architecture

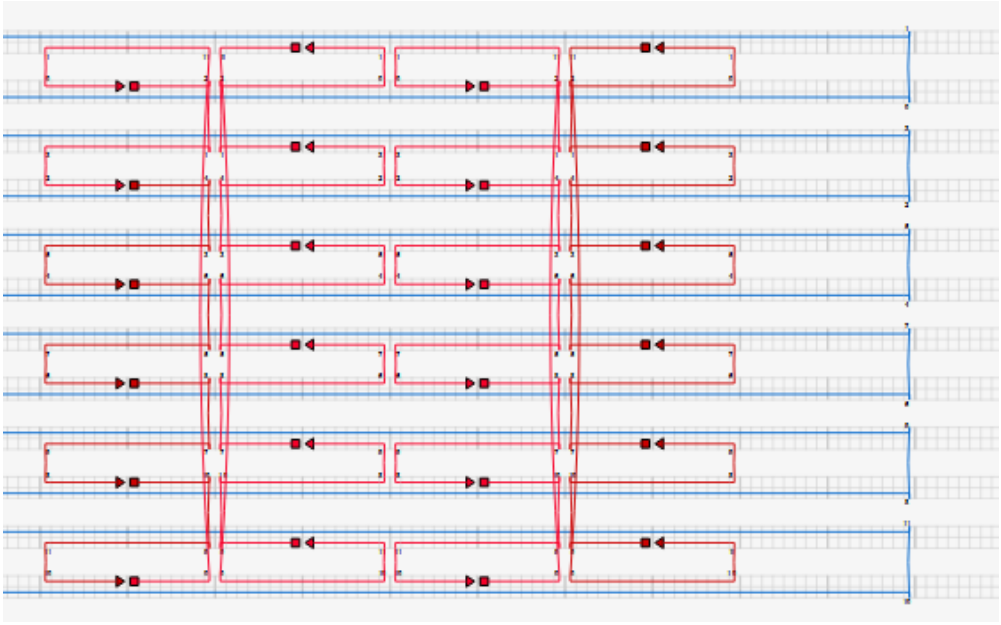

Figure 7: M13mp18 scaffold strand is in blue. Staple strands are in red.

Appendix 3: M13mp18 scaffold strand sequence

AATGCTACTACTATTAGTAGAATTGATGCCACCTTTTCAGCTCGCGCCCCAAATGAAAATATA
GCTAAACAGGTTATTGACCATTTGCGAAATGTATCTAATGGTCAAACTAAATCTACTCGTTCG
CAGAATTGGGAATCAACTGTTATATGGAATGAAACTTCCAGACACCGTACTTTAGTTGCATAT
TTAAAACATGTTGAGCTACAGCATTATATTCAGCAATTAAGCTCTAAGCCATCCGCAAAAATG
ACCTCTTATCAAAAGGAGCAATTAAAGGTACTCTCTAATCCTGACCTGTTGGAGTTTGCTTCCG
GTCTGGTTCGCTTTGAAGCTCGAATTAAAACGCGATATTTGAAGTCTTTCGGGCTTCCTCTTAA
TCTTTTTGATGCAATCCGCTTTGCTTCTGACTATAATAGTCAGGGTAAAGACCTGATTTTTGAT
TTATGGTCATTCTCGTTTTCTGAACTGTTTAAAGCATTTGAGGGGGATTCAATGAATATTTATG
ACGATTCCGCAGTATTGGACGCTATCCAGTCTAAACATTTTACTATTACCCCCTCTGGCAAAAC
TTCTTTTGCAAAAGCCTCTCGCTATTTTGGTTTTTATCGTCGTCTGGTAAACGAGGGTTATGAT
AGTGTTGCTCTTACTATGCCTCGTAATTCCTTTTGGCGTTATGTATCTGCATTAGTTGAATGTG
GTATTCCTAAATCTCAACTGATGAATCTTTCTACCTGTAATAATGTTGTTCCGTTAGTTCGTTTT
ATTAACGTAGATTTTTCTTCCCAACGTCCTGACTGGTATAATGAGCCAGTTCTTAAAATCGCAT
AAGGTAATTCACAATGATTAAAGTTGAAATTAAACCATCTCAAGCCCAATTTACTACTCGTTC
TGGTGTTTCTCGTCAGGGCAAGCCTTATTCACTGAATGAGCAGCTTTGTTACGTTGATTTGGGT
AATGAATATCCGGTTCTTGTCAAGATTACTCTTGATGAAGGTCAGCCAGCCTATGCGCCTGGT
CTGTACACCGTTCATCTGTCCTCTTTCAAAGTTGGTCAGTTCGGTTCCCTTATGATTGACCGTCT
GCGCCTCGTTCCGGCTAAGTAACATGGAGCAGGTCGCGGATTTCGACACAATTTATCAGGCGA
TGATACAAATCTCCGTTGTACTTTGTTTCGCGCTTGGTATAATCGCTGGGGGTCAAAGATGAGT
GTTTTAGTGTATTCTTTTGCCTCTTTCGTTTTAGGTTGGTGCCTTCGTAGTGGCATTACGTATTT
TACCCGTTTAATGGAAACTTCCTCATGAAAAAGTCTTTAGTCCTCAAAGCCTCTGTAGCCGTTG
CTACCCTCGTTCCGATGCTGTCTTTCGCTGCTGAGGGTGACGATCCCGCAAAAGCGGCCTTTA
ACTCCCTGCAAGCCTCAGCGACCGAATATATCGGTTATGCGTGGGCGATGGTTGTTGTCATTG
TCGGCGCAACTATCGGTATCAAGCTGTTTAAGAAATTCACCTCGAAAGCAAGCTGATAAACCG
ATACAATTAAAGGCTCCTTTTGGAGCCTTTTTTTTGGAGATTTTCAACGTGAAAAAATTATTAT
TCGCAATTCCTTTAGTTGTTCCTTTCTATTCTCACTCCGCTGAAACTGTTGAAAGTTGTTTAGCA
AAATCCCATACAGAAAATTCATTTACTAACGTCTGGAAAGACGACAAAACTTTAGATCGTTAC
GCTAACTATGAGGGCTGTCTGTGGAATGCTACAGGCGTTGTAGTTTGTACTGGTGACGAAACT
CAGTGTTACGGTACATGGGTTCCTATTGGGCTTGCTATCCCTGAAAATGAGGGTGGTGGCTCT
GAGGGTGGCGGTTCTGAGGGTGGCGGTTCTGAGGGTGGCGGTACTAAACCTCCTGAGTACGG
TGATACACCTATTCCGGGCTATACTTATATCAACCCTCTCGACGGCACTTATCCGCCTGGTACT
GAGCAAAACCCCGCTAATCCTAATCCTTCTCTTGAGGAGTCTCAGCCTCTTAATACTTTCATGT
TTCAGAATAATAGGTTCCGAAATAGGCAGGGGGCATTAACTGTTTATACGGGCACTGTTACTC
AAGGCACTGACCCCGTTAAAACTTATTACCAGTACACTCCTGTATCATCAAAAGCCATGTATG
ACGCTTACTGGAACGGTAAATTCAGAGACTGCGCTTTCCATTCTGGCTTTAATGAGGATTTATT
TGTTTGTGAATATCAAGGCCAATCGTCTGACCTGCCTCAACCTCCTGTCAATGCTGGCGGCGG
CTCTGGTGGTGGTTCTGGTGGCGGCTCTGAGGGTGGTGGCTCTGAGGGTGGCGGTTCTGAGGG
TGGCGGCTCTGAGGGAGGCGGTTCCGGTGGTGGCTCTGGTTCCGGTGATTTTGATTATGAAAA
GATGGCAAACGCTAATAAGGGGGCTATGACCGAAAATGCCGATGAAAACGCGCTACAGTCTG
ACGCTAAAGGCAAACTTGATTCTGTCGCTACTGATTACGGTGCTGCTATCGATGGTTTCATTGG
TGACGTTTCCGGCCTTGCTAATGGTAATGGTGCTACTGGTGATTTTGCTGGCTCTAATTCCCAA
ATGGCTCAAGTCGGTGACGGTGATAATTCACCTTTAATGAATAATTTCCGTCAATATTTACCTT
CCCTCCCTCAATCGGTTGAATGTCGCCCTTTTGTCTTTGGCGCTGGTAAACCATATGAATTTTC
TATTGATTGTGACAAAATAAACTTATTCCGTGGTGTCTTTGCGTTTCTTTTATATGTTGCCACCT
TTATGTATGTATTTTCTACGTTTGCTAACATACTGCGTAATAAGGAGTCTTAATCATGCCAGTT
CTTTTGGGTATTCCGTTATTATTGCGTTTCCTCGGTTTCCTTCTGGTAACTTTGTTCGGCTATCT
GCTTACTTTTCTTAAAAAGGGCTTCGGTAAGATAGCTATTGCTATTTCATTGTTTCTTGCTCTTA
TTATTGGGCTTAACTCAATTCTTGTGGGTTATCTCTCTGATATTAGCGCTCAATTACCCTCTGA
CTTTGTTCAGGGTGTTCAGTTAATTCTCCCGTCTAATGCGCTTCCCTGTTTTTATGTTATTCTCT
CTGTAAAGGCTGCTATTTTCATTTTTGACGTTAAACAAAAAATCGTTTCTTATTTGGATTGGGA
TAAATAATATGGCTGTTTATTTTGTAACTGGCAAATTAGGCTCTGGAAAGACGCTCGTTAGCG
TTGGTAAGATTCAGGATAAAATTGTAGCTGGGTGCAAAATAGCAACTAATCTTGATTTAAGGC
TTCAAAACCTCCCGCAAGTCGGGAGGTTCGCTAAAACGCCTCGCGTTCTTAGAATACCGGATA

AGCCTTCTATATCTGATTTGCTTGCTATTGGGCGCGGTAATGATTCCTACGATGAAAATAAAA
ACGGCTTGCTTGTTCTCGATGAGTGCGGTACTTGGTTTAATACCCGTTCTTGGAATGATAAGGA
AAGACAGCCGATTATTGATTGGTTTCTACATGCTCGTAAATTAGGATGGGATATTATTTTTCTT
GTTCAGGACTTATCTATTGTTGATAAACAGGCGCGTTCTGCATTAGCTGAACATGTTGTTTATT
GTCGTCGTCTGGACAGAATTACTTTACCTTTTGTCGGTACTTTATATTCTCTTATTACTGGCTCG
AAAATGCCTCTGCCTAAATTACATGTTGGCGTTGTTAAATATGGCGATTCTCAATTAAGCCCTA
CTGTTGAGCGTTGGCTTTATACTGGTAAGAATTTGTATAACGCATATGATACTAAACAGGCTTT
TTCTAGTAATTATGATTCCGGTGTTTATTCTTATTTAACGCCTTATTTATCACACGGTCGGTATT
TCAAACCATTAAATTTAGGTCAGAAGATGAAATTAACTAAAATATATTTGAAAAAGTTTTCTC
GCGTTCTTTGTCTTGCGATTGGATTTGCATCAGCATTTACATATAGTTATATAACCCAACCTAA
GCCGGAGGTTAAAAAGGTAGTCTCTCAGACCTATGATTTTGATAAATTCACTATTGACTCTTCT
CAGCGTCTTAATCTAAGCTATCGCTATGTTTTCAAGGATTCTAAGGGAAAATTAATTAATAGC
GACGATTTACAGAAGCAAGGTTATTCACTCACATATATTGATTTATGTACTGTTTCCATTAAAA
AAGGTAATTCAAATGAAATTGTTAAATGTAATTAATTTTGTTTTCTTGATGTTTGTTTCATCAT
CTTCTTTTGCTCAGGTAATTGAAATGAATAATTCGCCTCTGCGCGATTTTGTAACTTGGTATTC
AAAGCAATCAGGCGAATCCGTTATTGTTTCTCCCGATGTAAAAGGTACTGTTACTGTATATTC
ATCTGACGTTAAACCTGAAAATCTACGCAATTTCTTTATTTCTGTTTTACGTGCAAATAATTTT
GATATGGTAGGTTCTAACCCTTCCATTATTCAGAAGTATAATCCAAACAATCAGGATTATATT
GATGAATTGCCATCATCTGATAATCAGGAATATGATGATAATTCCGCTCCTTCTGGTGGTTTCT
TTGTTCCGCAAAATGATAATGTTACTCAAACTTTTAAAATTAATAACGTTCGGGCAAAGGATT
TAATACGAGTTGTCGAATTGTTTGTAAAGTCTAATACTTCTAAATCCTCAAATGTATTATCTAT
TGACGGCTCTAATCTATTAGTTGTTAGTGCTCCTAAAGATATTTTAGATAACCTTCCTCAATTC
CTTTCAACTGTTGATTTGCCAACTGACCAGATATTGATTGAGGGTTTGATATTTGAGGTTCAGC
AAGGTGATGCTTTAGATTTTTCATTTGCTGCTGGCTCTCAGCGTGGCACTGTTGCAGGCGGTGT
TAATACTGACCGCCTCACCTCTGTTTTATCTTCTGCTGGTGGTTCGTTCGGTATTTTTAATGGCG
ATGTTTTAGGGCTATCAGTTCGCGCATTAAAGACTAATAGCCATTCAAAAATATTGTCTGTGC
CACGTATTCTTACGCTTTCAGGTCAGAAGGGTTCTATCTCTGTTGGCCAGAATGTCCCTTTTAT
TACTGGTCGTGTGACTGGTGAATCTGCCAATGTAAATAATCCATTTCAGACGATTGAGCGTCA
AAATGTAGGTATTTCCATGAGCGTTTTTCCTGTTGCAATGGCTGGCGGTAATATTGTTCTGGAT
ATTACCAGCAAGGCCGATAGTTTGAGTTCTTCTACTCAGGCAAGTGATGTTATTACTAATCAA
AGAAGTATTGCTACAACGGTTAATTTGCGTGATGGACAGACTCTTTTACTCGGTGGCCTCACT
GATTATAAAAACACTTCTCAGGATTCTGGCGTACCGTTCCTGTCTAAAATCCCTTTAATCGGCC
TCCTGTTTAGCTCCCGCTCTGATTCTAACGAGGAAAGCACGTTATACGTGCTCGTCAAAGCAA
CCATAGTACGCGCCCTGTAGCGGCGCATTAAGCGCGGCGGGTGTGGTGGTTACGCGCAGCGT
GACCGCTACACTTGCCAGCGCCCTAGCGCCCGCTCCTTTCGCTTTCTTCCCTTCCTTTCTCGCCA
CGTTCGCCGGCTTTCCCCGTCAAGCTCTAAATCGGGGGCTCCCTTTAGGGTTCCGATTTAGTGC
TTTACGGCACCTCGACCCCAAAAAACTTGATTTGGGTGATGGTTCACGTAGTGGGCCATCGCC
CTGATAGACGGTTTTTCGCCCTTTGACGTTGGAGTCCACGTTCTTTAATAGTGGACTCTTGTTC
CAAACTGGAACAACACTCAACCCTATCTCGGGCTATTCTTTTGATTTATAAGGGATTTTGCCGA
TTTCGGAACCACCATCAAACAGGATTTTCGCCTGCTGGGGCAAACCAGCGTGGACCGCTTGCT
GCAACTCTCTCAGGGCCAGGCGGTGAAGGGCAATCAGCTGTTGCCCGTCTCACTGGTGAAAA
GAAAAACCACCCTGGCGCCCAATACGCAAACCGCCTCTCCCCGCGCGTTGGCCGATTCATTAA
TGCAGCTGGCACGACAGGTTTCCCGACTGGAAAGCGGGCAGTGAGCGCAACGCAATTAATGT
GAGTTAGCTCACTCATTAGGCACCCCAGGCTTTACACTTTATGCTTCCGGCTCGTATGTTGTGT
GGAATTGTGAGCGGATAACAATTTCACACAGGAAACAGCTATGACCATGATTACGAATTCGA
GCTCGGTACCCGGGGATCCTCTAGAGTCGACCTGCAGGCATGCAAGCTTGGCACTGGCCGTCG
TTTTACAACGTCGTGACTGGGAAAACCCTGGCGTTACCCAACTTAATCGCCTTGCAGCACATC
CCCCTTTCGCCAGCTGGCGTAATAGCGAAGAGGCCCGCACCGATCGCCCTTCCCAACAGTTGC
GCAGCCTGAATGGCGAATGGCGCTTTGCCTGGTTTCCGGCACCAGAAGCGGTGCCGGAAAGC
TGGCTGGAGTGCGATCTTCCTGAGGCCGATACTGTCGTCGTCCCCTCAAACTGGCAGATGCAC
GGTTACGATGCGCCCATCTACACCAACGTGACCTATCCCATTACGGTCAATCCGCCGTTTGTTC
CCACGGAGAATCCGACGGGTTGTTACTCGCTCACATTTAATGTTGATGAAAGCTGGCTACAGG
AAGGCCAGACGCGAATTATTTTTGATGGCGTTCCTATTGGTTAAAAAATGAGCTGATTTAACA
AAAATTTAATGCGAATTTTAACAAAATATTAACGTTTACAATTTAAATATTTGCTTATACAATC
TTCCTGTTTTTGGGGCTTTTCTGATTATCAACCGGGGTACATATGATTGACATGCTAGTTTTAC
GATTACCGTTCATCGATTCTCTTGTTTGCTCCAGACTCTCAGGCAATGACCTGATAGCCTTTGT

AGATCTCTCAAAAATAGCTACCCTCTCCGGCATTAATTTATCAGCTAGAACGGTTGAATATCA
TATTGATGGTGATTTGACTGTCTCCGGCCTTTCTCACCCTTTTGAATCTTTACCTACACATTACT
CAGGCATTGCATTTAAAATATATGAGGGTTCTAAAAATTTTTATCCTTGCGTTGAAATAAAGG
CTTCTCCCGCAAAAGTATTACAGGGTCATAATGTTTTTGGTACAACCGATTTAGCTTTATGCTC
TGAGGCTTTATTGCTTAATTTTGCTAATTCTTTGCCTTGCCTGTATGATTTATTGGATGTT

Appendix 4: RT A seed staple sequences

T_3R2F_HP:	TGTAGCATAACTTTCAGGCATCCGTTTTCGGATGCCTTACAGTTTCTAATTGTA
T_3R4F_HP:	TCGGTTTAGGTCGCTGGCTGACGCTTTTGCGTCAGCTTAGGCTTGCAAAGACTT
T_3R6F_HP:	TTTCATGATGACCCCCACCAGCCGTTTTCGGCTGGTTTAGCGATTAAGGCGCAG
T_3R8F_HP:	ACGGTCAATGACAAGACGGAGGCGTTTTCGCCTCCGTTACCGGATATGGTTTAA
T_3R10F_HP:	TTTCAACTACGGAACACTCGCTGCTTTTGCAGCGAGTTACATTATTAACACTAT
T_3R12F_CYC_HP:	CATAACCCACCGCCACCTGGCTCGTTTTCGAGCCAGTTCCTCAGAAACAACGCC
T_3R2E_HP:	TGCTAAACTCCACAGAGCCAGTGCTTTTGCACTGGCTTCAGCCCTCTACCGCCA
T_3R4E_HP:	ATATATTCTCAGCTTGCCGTCCGCTTTTGCGGACGGTTCTTTCGAGTGGGATTT
T_3R6E_HP:	CTCATCTTGGAAGTTTCGGATGGCTTTTGCCATCCGTTCCATTAAACATAACCG
T_3R8E_HP:	AGTAATCTTCATAAGGTCTGGTCGTTTTCGACCAGATTGAACCGAACTAAAACA
T_3R10E_HP:	ACGAACTATTAATCATGGCACCTGTTTTCAGGTGCCTTTGTGAATTTCATCAAG
T_3R12E_CYC_HP:	CCCTCAGATCGTTTACCGCTTGCGTTTTCGCAAGCGTTCAGACGACTTAATAAA
T_5R2F_HP:	TGAGTTTCAAAGGAACGTCCACCGTTTTCGGTGGACTTAACTAAAGATCTCCAA
T_5R4F_HP:	AAAAAAGGCTTTTGCGGTGGTCCGTTTTCGGACCACTTGGATCGTCGGGTAGCA
T_5R6F_HP:	ACGGCTACAAGTACAACTCGGCACTTTTGTGCCGAGTTCGGAGATTCGCGACCT
T_5R8F_HP:	GCTCCATGACGTAACACGGATCGCTTTTGCGATCCGTTAAGCTGCTACACCAGA
T_5R10F_HP:	ACGAGTAGATCAGTTGCACCGCTGTTTTCAGCGGTGTTAGATTTAGCGCCAAAA
T_5R12F_CYC_HP:	GGAATTACCACCACCCGTGAGGCGTTTTCGCCTCACTTTCATTTTCCGTAACAC
T_5R2E_HP:	GAGAATAGGTCACCAGCGGAACCGTTTTCGGTTCCGTTTACAAACTCCGCCACC
T_5R4E_HP:	AAAGGCCGCTCCAAAACCGTGGCGTTTTCGCCACGGTTGGAGCCTTAGCGGAGT
T_5R6E_HP:	GCGAAACAAGAGGCTTGTGCTGCGTTTTCGCAGCACTTTGAGGACTAGGGAGTT
T_5R8E_HP:	CCAAATCATTACTTAGACGCTGGCTTTTGCCAGCGTTTCCGGAACGTACCAAGC
T_5R10E_HP:	AAAGATTCTAAATTGGCGACGGACTTTTGTCCGTCGTTGCTTGAGATTCATTAC
T_5R12E_CYC_HP:	CTCAGAGCGAGGCATAGGCTCCGCTTTTGCGGAGCCTTGTAAGAGCACAGGTAG

Hairpins are highlighted in red.

Appendix 5: RT A seed adapter sequences

A-4bp-1REd_1:	CAGCCAAGACGCAGGTAGCGAGACAGAGCTGAAAGTATTAAGAGG
A-4bp-1_2REd_3:	TCGCTACCTGCGTTCGTCGGATGGTGAGGTCCACGCTCTGTC
A-4bp-1_2REd_5:	CTATTATTCTGAAACAGTGGACCTCACCATCCGACGACACGAGCA
A-4bp-2REd_2:	TGGTTGCTCGTGCTTGGCTGGCAT
A-4bp-3SEd_1:	CACGGAGTCGAAGCGTAGGACGGTAGCCAGTCAGACGATTGGCCT
A-4bp-3_4SEd_3:	GTCCTACGCTTCGGACCTTGGTGATGCTGGACTGTGGCTACC
A-4bp-4SEd_5:	CAGGAGGTTGAGGCAGCAGTCCAGCATCACCAAGGTCGCTCGGCA
A-4bp-3_4SEd_2:	TCTGTGCCGAGCACTCCGTGAGGT
A-4bp-5REd_1:	CAGAGCCACGGCATGGTCTTGCGTTGGAGGCGTCAGACTGTAGCG
A-4bp-5_6REd_3:	CAAGACCATGCCGACCTCATCCTCGCTTTCGGTGCTCCAACG
A-4bp-6REd_5:	ATCAAGTTTGCCTTTACACCGAAAGCGAGGATGAGGTGCGGACGA
A-4bp-5_6REd_2:	TGGTTCGTCCGCTGGCTCTGGCAT
A-4bp-7SEd_1:	CACGGAGTCTACGGCAGTGACCGATCTCCAGACAAAAGGGCGACA
A-4bp-7_8SEd_3:	GTCACTGCCGTAGCTCACGAGGCACAACCACAGCGGAGATCG
A-4bp-8SEd_5:	GGTTTACCAGCGCCAAGCTGTGGTTGTGCCTCGTGAGGCTCGGCA
A-4bp-7_8SEd_2:	TCTGTGCCGAGCACTCCGTGAGGT
A-4bp-9REd_1:	CAACCGTCGTTCCACAGGACTCGCACTTCGCAGATAGCCGAACAA
A-4bp-9_10REd_3:	AGTCCTGTGGAACACCACGAGACGCCATCGAGCGGAAGTGCG
A-4bp-10SRd_5:	TTTTTAAGAAAAGTAACGCTCGATGGCGTCTCGTGGTAAGCCTGA
A-4bp-9_10SRd_2:	TGGTTCAGGCTTGACGGTTGGCAT
A-4bp-11SEd_1:	CACGGAGTCAAGGCTACGAGTCAGACAGGAACGTCAAAAATGAAA
A-4bp-11_12SEd_3:	ACTCGTAGCCTTGGACCGCACTCACCACTGCTCGCCTGTCTG
A-4bp-12SEd_5:	AAACGATTTTTTGTTTCGAGCAGTGGTGAGTGCGGTCGCTCGGCA
A-4bp-11_12SEd_2:	TCTGTGCCGAGCACTCCGTGAGGT

Appendix 6: Schematic of RT A seed adapter complexes

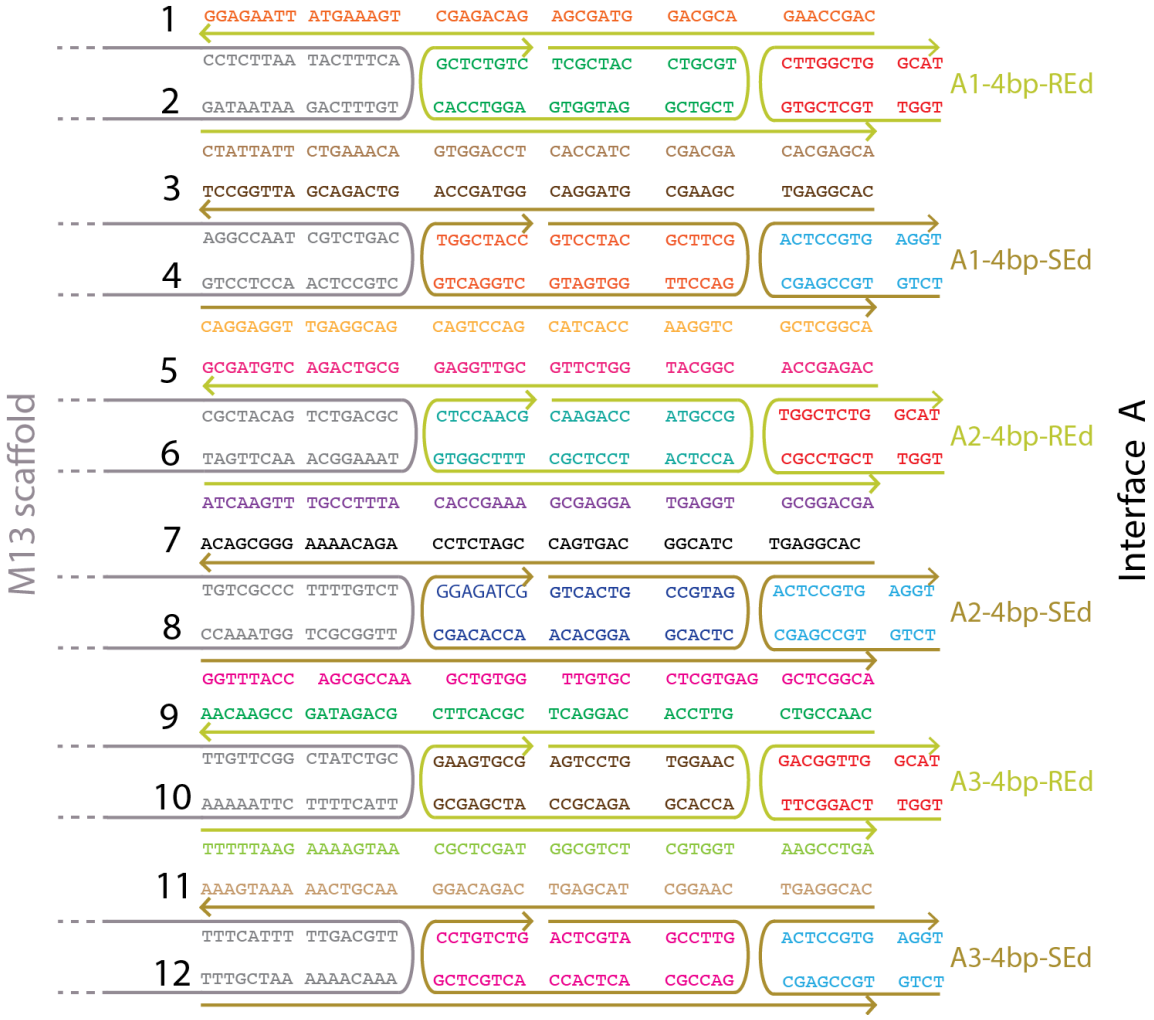

Figure 8: M13mp18 scaffold strand represented in gray. REd and SEd adapter complexes alternate. *[33]*

Appendix 7: Modified DNA RT A seed adapter sequences

A-4bp-1REd_1:	CAGCCAAGACGCAGGTAGCGAGACAGAGCTGAAAGTATTAAGAGG
A-4bp-1_2REd_3:	TCGCTACCTGCGTTCGTCGGATGGTGAGGTCCACGCTCTGTC
A-4bp-1_2REd_5:	CTATTATTCTGAAACAGTGGACCTCACCATCCGACGACACGAGCA
A-4bp-2REd_2:	TGGTTGCTCGTGCTTGGCTGGCAT
A-4bp-3SEd_1:	CACGGAGTCGAAGCGTAGGACGGTAGCCAGTCAGACGATTGGCCT
A-4bp-3_4SEd_3:	GTCCTACGCTTCGGACCTTGGTGATGCTGGACTGTGGCTACC
A-4bp-4SEd_5:	CAGGAGGTTGAGGCAGCAGTCCAGCATCACCAAGGTCGCTCGGCA
A-4bp-3_4SEd_2:	TCTGTGCCGAGCACTCCGTGAGGT
A-4bp-5REd_1:	**CAGCCAAGCGGCATGGTCTTGCGTTGGAGGCGTCAGACTGTAGCG**
A-4bp-5_6REd_3:	CAAGACCATGCCGACCTCATCCTCGCTTTCGGTGCTCCAACG
A-4bp-6REd_5:	**ATCAAGTTTGCCTTTACACCGAAAGCGAGGATGAGGTCACGAGCA**
A-4bp-5_6REd_2:	**TGGTTGCTCGTGCTTGGCTGGCAT**
A-4bp-7SEd_1:	CACGGAGTCTACGGCAGTGACCGATCTCCAGACAAAAGGGCGACA
A-4bp-7_8SEd_3:	GTCACTGCCGTAGCTCACGAGGCACAACCACAGCGGAGATCG
A-4bp-8SEd_5:	GGTTTACCAGCGCCAAGCTGTGGTTGTGCCTCGTGAGGCTCGGCA
A-4bp-7_8SEd_2:	TCTGTGCCGAGCACTCCGTGAGGT
A-4bp-9REd_1:	**CAGCCAAGGTTCCACAGGACTCGCACTTCGCAGATAGCCGAACAA**
A-4bp-9_10REd_3:	AGTCCTGTGGAACACCACGAGACGCCATCGAGCGGAAGTGCG
A-4bp-10SRd_5:	**TTTTTAAGAAAAGTAACGCTCGATGGCGTCTCGTGGTCACGAGCA**
A-4bp-9_10SRd_2:	**TGGTTGCTCGTGCTTGGCTGGCAT**
A-4bp-11SEd_1:	CACGGAGTCAAGGCTACGAGTCAGACAGGAACGTCAAAAATGAAA
A-4bp-11_12SEd_3:	ACTCGTAGCCTTGGACCGCACTCACCACTGCTCGCCTGTCTG
A-4bp-12SEd_5:	AAACGATTTTTTGTTTCGAGCAGTGGTGAGTGCGGTCGCTCGGCA
A-4bp-11_12SEd_2:	TCTGTGCCGAGCACTCCGTGAGGT

Bolded items are modified strands.

Appendix 8: RNA RT A seed adapter sequences

A-4bp-1REd_1:	CAGCCAAGACGCAGGTAGCGAGACAGAGCTGAAAGTATTAAGAGG
A-4bp-1_2REd_3:	TCGCTACCTGCGTTCGTCGGATGGTGAGGTCCACGCTCTGTC
A-4bp-1_2REd_5:	CTATTATTCTGAAACAGTGGACCTCACCATCCGACGACACGAGCA
A-4bp-2REd_2:	TGGTTGCTCGTGCTTGGCTGGCAT
A-4bp-3SEd_1:	CACGGAGTCGAAGCGTAGGACGGTAGCCAGTCAGACGATTGGCCT
A-4bp-3_4SEd_3:	GTCCTACGCTTCGGACCTTGGTGATGCTGGACTGTGGCTACC
A-4bp-4SEd_5:	CAGGAGGTTGAGGCAGCAGTCCAGCATCACCAAGGTCGCTCGGCA
A-4bp-3_4SEd_2:	TCTGTGCCGAGCACTCCGTGAGGT
A-4bp-5REd_1:	**CAGCCAAGCGGCATGGTCTTGCGTTGGAGGCGTCAGACTGTAGCG**
A-4bp-5_6REd_3:	CAAGACCATGCCGACCTCATCCTCGCTTTCGGTGCTCCAACG
A-4bp-6REd_5:	**ATCAAGTTTGCCTTTACACCGAAAGCGAGGATGAGGTCACGAGCA**
A-4bp-5_6REd_2:	**UGGUUGCUCGUGCUUGGCUGGCAU**
A-4bp-7SEd_1:	CACGGAGTCTACGGCAGTGACCGATCTCCAGACAAAAGGGCGACA
A-4bp-7_8SEd_3:	GTCACTGCCGTAGCTCACGAGGCACAACCACAGCGGAGATCG
A-4bp-8SEd_5:	GGTTTACCAGCGCCAAGCTGTGGTTGTGCCTCGTGAGGCTCGGCA
A-4bp-7_8SEd_2:	TCTGTGCCGAGCACTCCGTGAGGT
A-4bp-9REd_1:	**CAGCCAAGGTTCCACAGGACTCGCACTTCGCAGATAGCCGAACAA**
A-4bp-9_10REd_3:	AGTCCTGTGGAACACCACGAGACGCCATCGAGCGGAAGTGCG
A-4bp-10SRd_5:	**TTTTTAAGAAAAGTAACGCTCGATGGCGTCTCGTGGTCACGAGCA**
A-4bp-9_10SRd_2:	**UGGUUGCUCGUGCUUGGCUGGCAU**
A-4bp-11SEd_1:	CACGGAGTCAAGGCTACGAGTCAGACAGGAACGTCAAAAATGAAA
A-4bp-11_12SEd_3:	ACTCGTAGCCTTGGACCGCACTCACCACTGCTCGCCTGTCTG
A-4bp-12SEd_5:	AAACGATTTTTTGTTTCGAGCAGTGGTGAGTGCGGTCGCTCGGCA
A-4bp-11_12SEd_2:	TCTGTGCCGAGCACTCCGTGAGGT

Bolded items are modified strands.

Appendix 9: Rigid Cap architecture

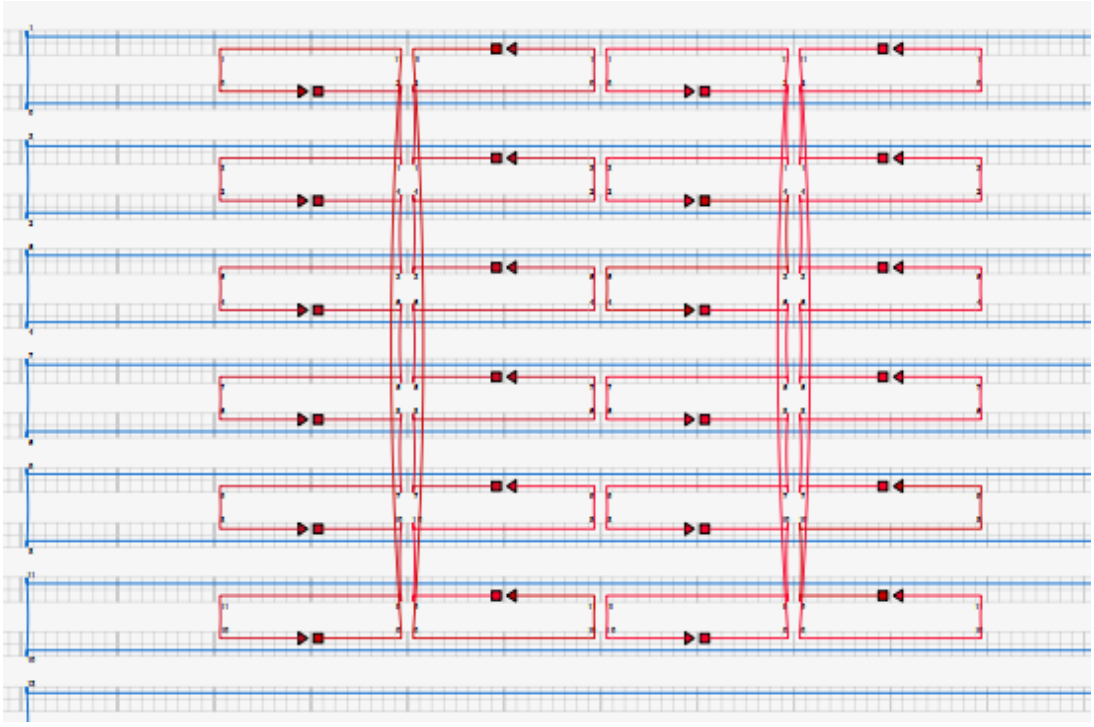

Figure 9: M13mp18 scaffold strand is in blue. Staple strands are in red.

Appendix 10: Rigid Cap staple sequences

T5R2F_HP:	AATGCCCCATAAATCCGCTCGGACTTTTGTCCGAGCTTTCATTAAAAGAACCAC
T5R4F_HP:	CACCAGAGTTCGGTCAGCCGAGCGTTTTCGCTCGGCTTTAGCCCCCTCGATAGC
T5R6F_HP:	AGCACCGTAGGGAAGGTCGGAGGCTTTTGCCTCCGATTTAAATATTTTATTTTG
T5R8F_HP:	TCACAATCCCGAGGAACTGGTGGCTTTTGCCACCAGTTACGCAATAATGAAATA
T5R10F_HP:	GCAATAGCAGAGAATACCGCAGGCTTTTGCCTGCGGTTACATAAAAACAGCCAT
T5R12F_CYC_HP:	ATTATTTAGAAGGATTGCCATCGCTTTTGCGATGGCTTAGGATTAGAAACAGTT
T5R2E_HP:	ACAAACAACTGCCTATCACGACGCTTTTGCGTCGTGTTTTCGGAACCTGAGACT
T5R4E_HP:	TCGGCATTCCGCCGCCGTCGCTGCTTTTGCAGCGACTTAGCATTGATGATATTC
T5R6E_HP:	ATTGAGGGAATCAGTACGGAGCACTTTTGTGCTCCGTTGCGACAGACGTTTTCA
T5R8E_HP:	GAAGGAAAAATAGAAAGCCTAGCGTTTTCGCTAGGCTTATTCATATTTCAACCG
T5R10E_HP:	CTTTACAGTATCTTACCGCTCGTGTTTTCACGAGCGTTCGAAGCCCAGTTACCA
T5R12E_CYC_HP:	CCTCAAGATCCCAATCCGTGGAGCTTTTGCTCCACGTTCAAATAAGATAGCAGC
T3R2F_HP:	TGCCTTGACAGTCTCTGTCGGTGCTTTTGCACCGACTTGAATTTACCCCTCAGA
T3R4F_HP:	GCCACCACTCTTTTCACGGTCGGCTTTTGCCGACCGTTTAATCAAATAGCAAGG
T3R6F_HP:	CCGGAAACTAAAGGTGGACCTGGCTTTTGCCAGGTCTTAATTATCATAAAAGAA
T3R8F_HP:	ACGCAAAGAAGAACTGTCGGCTCGTTTTCGAGCCGATTGCATGATTTGAGTTAA
T3R10F_HP:	GCCCAATAGACGGGAGCACAGGCGTTTTCGCCTGTGTTAATTAACTTTCCAGAG
T3R12F_CYC_HP:	CCTAATTTACCAGGCGTCGGAGCGTTTTCGCTCCGATTGATAAGTGGGGGTCAG

T3R2E_HP:	GGAAAGCGGTAACAGTGTGGCAGCTTTTGCTGCCACTTGCCCGTATCGGGGTTT
T3R4E_HP:	GTTTGCCACCTCAGAGACCAGGCGTTTTCGCCTGGTTTCCGCCACCGCCAGAAT
T3R6E_HP:	TTATTCATGTCACCAAGCTCGCTGTTTTCAGCGAGCTTTGAAACCATTATTAGC
T3R8E_HP:	ATACCCAAACACCACGCCTACCGCTTTTGCGGTAGGTTGAATAAGTGACGGAAA
T3R10E_HP:	GCGCATTAATAAGAGCCTGGACGCTTTTGCGTCCAGTTAAGAAACAATAACGGA

Hairpins are highlighted in red.

Appendix 11: Other cap architectures

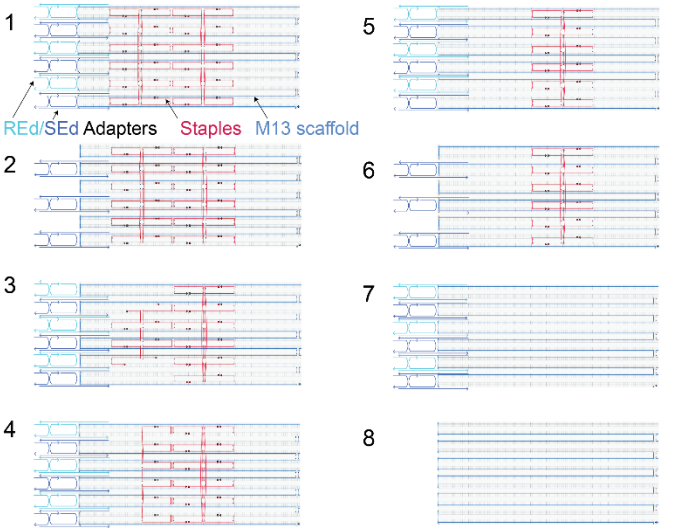

Cap Type	% of caps nucleating nanotubes in the absence of RT A Seeds	% of RT A Seeded nanotubes capped
1 (Rigid Cap)	73.8 ± 4	96.1 ± 1
2	3.1 ± 0.3	64.3 ± 2.4
3	15 ± 4.3	90.7 ± 1.8
4	1.5 ± 0.6	93.7 ± 1.9
5	4.1 ± 0.9	87.6 ± 2.2
6	1.2 ± 0.2	33.3 ± 2.2
7 (Flexible Cap)	1.2 ± 1.2	88.6 ± 1.5
8 (Scaffold Only)	0	3.6 ± 0.9

Figure 10: Architectures 1 through 8 show different cap designs. The table on the right shows the percent of caps nucleating nanotubes and the percent of RT A seeded nanotubes capped. *[33]*

Appendix 12: Cap adapter sequences

B-4bp-1REd_1:	AGGGATAGCAAGCCCACAACGTGAGGACACTTGGAGGCTGCACTCG
B-4bp-1_2REd_3:	TGTCCTCACGTTGCTGGATGCCGATCCTACGACACCTCCAAG
B-4bp-2REd_5:	TCGCTGACTTGTCGTAGGATCGGCATCCAGATAGGAACCCATGTAC
B-4bp-1_2REd_4:	CAGACGAGTGCAGAGTCAGCGAATGC
B-4bp-3SEd_1:	GAATTGCGAATAATAAGTGACCTTGCTGTACCGTCGAGATGGAGTC
B-4bp-3_4SEd_3:	ACAGCAAGGTCACCGCAGTTGGCACTAGGCGACATCGACGGT
B-4bp-4SEd_5:	ACCACAACCTGTCGCCTAGTGCCAACTGCGTTTTTTCACGTTGAAA
B-4bp-3_4SEd_4:	ACCAGACTCCATCGGTTGTGGTACCT
B-4bp-5REd_1:	ACCCTCAGCAGCGAAACGAGTACGGCAACACGGTGAGAGCCTACGG
B-4bp-5_6REd_3:	GTTGCCGTACTCGACTGGTCACGAACGTCTCCAACTCACCGT
B-4bp-6REd_5:	TGCTCTGCCTTGGAGACGTTCGTGACCAGTGACAGCATCGGAACGA
B-4bp-5_6REd_4:	CAGACCGTAGGCTGGCAGAGCAATGC
B-4bp-7SEd_1:	TGTATCATCGCCTGATCAACGGTACGAGATGCGAAGCACAGAGTGC
B-4bp-7_8SEd_3:	TCTCGTACCGTTGCCAGTAGACCTAGCCGACGTGGCTTCGCA
B-4bp-8SEd_5:	AGTCACGCTCACGTCGGCTAGGTCTACTGGAAATTGTGTCGAAATC
B-4bp-7_8SEd_4:	ACCAGCACTCTGTAGCGTGACTACCT
B-4bp-9REd_1:	CATTCAGTGAATAAGGACGCTATGCCTATCGCTCTAGGACCTCTGG
B-4bp-9_10REd_3:	ATAGGCATAGCGTTGCTCCAGTCTGCTGCTCAGGCTAGAGCG
B-4bp-10REd_5:	TCCACGACTCCTGAGCAGCAGACTGGAGCACTTGCCCTGACGAGAA
B-4bp-9_10REd_4:	CAGACCAGAGGTCAGTCGTGGAATGC
B-4bp-11SEd_1:	GAATACCACATTCAACACCGATGAGGATCACGGCACTCGACACTGC
B-4bp-11_12SEd_3:	GATCCTCATCGGTCAAGCGAAGGTGCGAGCCTGTAGTGCCGT
B-4bp-12SEd_5:	AGCGGACTGACAGGCTCGCACCTTCGCTTGTAATGCAGATACATAA
B-4bp-11_12SEd_4:	ACCAGCAGTGTCGCAGTCCGCTACCT

Appendix 13: Schematic of cap adapter complexes

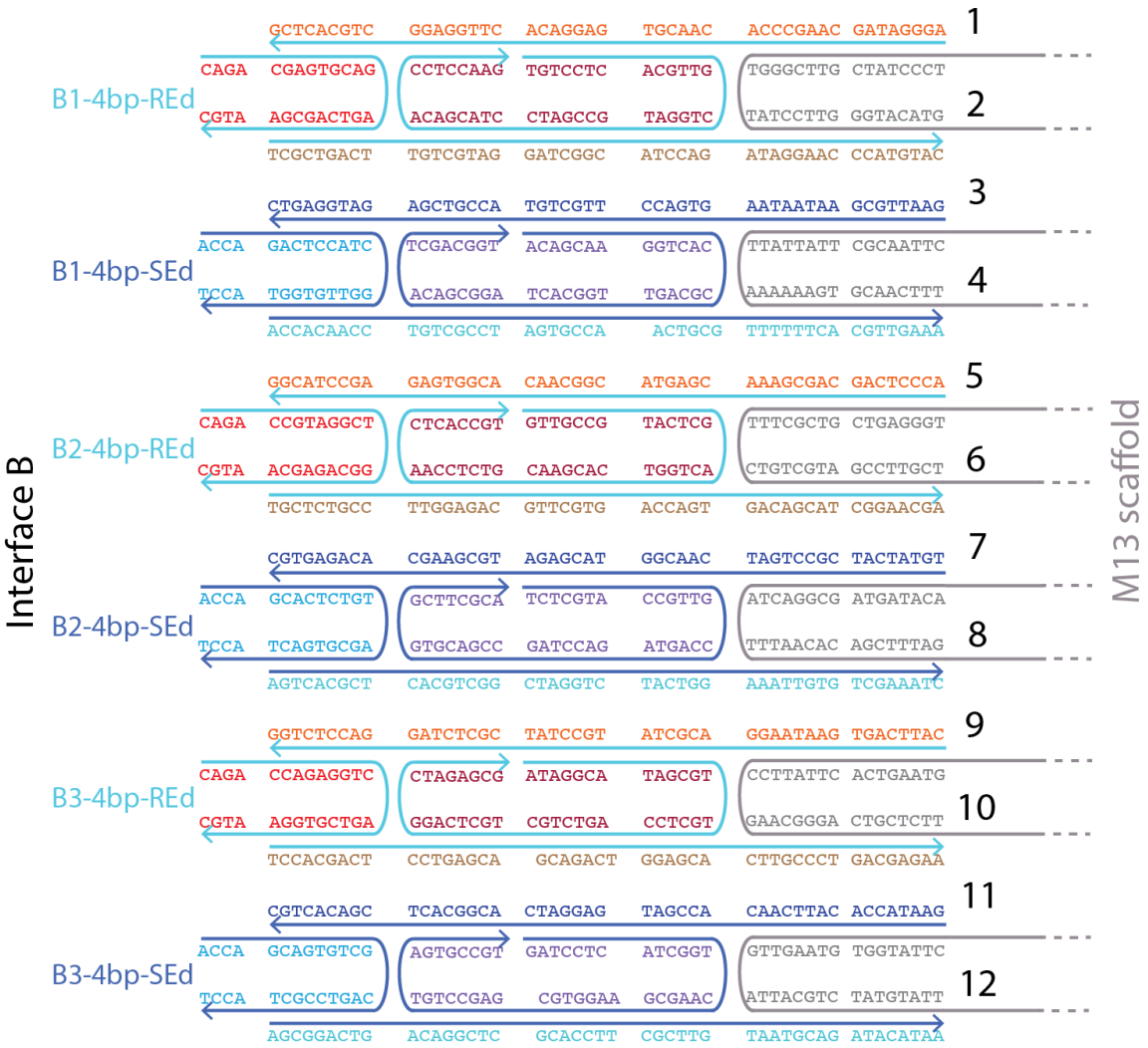

Figure 11: M13mp18 scaffold strand represented in gray. REd and SEd adapter complexes alternate. *[33]*

Appendix 14: Attachment and labelling strands

Labeling strand sequences

Labeling_strand_ATTO647N_seed_A	/5ATTO647NN/AAGCGTAGTCGGATCTC
Labeling_strand_ATTO488_cap	/5ATTO488N/AAGCGTAGTCGGATCTC

Attachment strand sequences

Unused_m13mp18_01	AAATTCTTACCAGTATAAAGCCAACTTTTGAGATCCGACTACGC
Unused_m13mp18_02	GCCTGTTTAGTATCATATGCGTTATTTTTGAGATCCGACTACGC
Unused_m13mp18_03	ACACCGGAATCATAATTACTAGAAATTTTGAGATCCGACTACGC
Unused_m13mp18_04	GATAAATAAGGCGTTAAATAAGAATTTTTGAGATCCGACTACGC
Unused_m13mp18_05	TTTAATGGTTTGAAATACCGACCGTTTTTGAGATCCGACTACGC
Unused_m13mp18_06	TTAGTTAATTTCATCTTCTGACCTATTTTGAGATCCGACTACGC
Unused_m13mp18_07	ACGCGAGAAAACTTTTTCAAATATATTTTGAGATCCGACTACGC
Unused_m13mp18_08	GATGCAAATCCAATCGCAAGACAAATTTTGAGATCCGACTACGC
Unused_m13mp18_09	TGGGTTATATAACTATATGTAAATGTTTTGAGATCCGACTACGC
Unused_m13mp18_10	ACTACCTTTTTAACCTCCGGCTTAGTTTTGAGATCCGACTACGC
Unused_m13mp18_11	AATTTATCAAAATCATAGGTCTGAGTTTTGAGATCCGACTACGC
Unused_m13mp18_12	TTAAGACGCTGAGAAGAGTCAATAGTTTTGAGATCCGACTACGC
Unused_m13mp18_13	TCCTTGAAAACATAGCGATAGCTTATTTTGAGATCCGACTACGC
Unused_m13mp18_14	TCGCTATTAATTAATTTTCCCTTAGTTTTGAGATCCGACTACGC
Unused_m13mp18_15	AGTGAATAACCTTGCTTCTGTAAATTTTTGAGATCCGACTACGC
Unused_m13mp18_16	GAAACAGTACATAAATCAATATATGTTTTGAGATCCGACTACGC
Unused_m13mp18_17	ATTTCATTTGAATTACCTTTTTTAATTTTGAGATCCGACTACGC
Unused_m13mp18_18	AGAAAACAAAATTAATTACATTTAATTTTGAGATCCGACTACGC
Unused_m13mp18_19	CAAAAGAAGATGATGAAACAAACATTTTTGAGATCCGACTACGC
Unused_m13mp18_20	GCGAATTATTCATTTCAATTACCTGTTTTGAGATCCGACTACGC
Unused_m13mp18_21	AATACCAAGTTACAAAATCGCGCAGTTTTGAGATCCGACTACGC
Unused_m13mp18_22	CAATAACGGATTCGCCTGATTGCTTTTTTGAGATCCGACTACGC
Unused_m13mp18_23	TAACAGTACCTTTTACATCGGGAGATTTTGAGATCCGACTACGC
Unused_m13mp18_24	CAGGTTTAACGTCAGATGAATATACTTTTGAGATCCGACTACGC
Unused_m13mp18_25	CAGAAATAAAGAAATTGCGTAGATTTTTTGAGATCCGACTACGC
Unused_m13mp18_26	CCATATCAAAATTATTTGCACGTAATTTTGAGATCCGACTACGC

Unused_m13mp18_27	TCTGAATAATGGAAGGGTTAGAACCTTTTGAGATCCGACTACGC
Unused_m13mp18_28	TATAATCCTGATTGTTTGGATTATATTTTGAGATCCGACTACGC
Unused_m13mp18_29	GATTATCAGATGATGGCAATTCATCTTTTGAGATCCGACTACGC
Unused_m13mp18_30	AAGGAGCGGAATTATCATCATATTCTTTTGAGATCCGACTACGC
Unused_m13mp18_31	CATTTTGCGGAACAAAGAAACCACCTTTTGAGATCCGACTACGC
Unused_m13mp18_32	TAATTTTAAAAGTTTGAGTAACATTTTTTGAGATCCGACTACGC
Unused_m13mp18_33	GTATTAAATCCTTTGCCCGAACGTTTTTTGAGATCCGACTACGC
Unused_m13mp18_34	TAGACTTTACAAACAATTCGACAACTTTTGAGATCCGACTACGC
Unused_m13mp18_35	ATAATACATTTGAGGATTTAGAAGTTTTTGAGATCCGACTACGC
Unused_m13mp18_36	CAACTAATAGATTAGAGCCGTCAATTTTTGAGATCCGACTACGC
Unused_m13mp18_37	TATCTAAAATATCTTTAGGAGCACTTTTTGAGATCCGACTACGC
Unused_m13mp18_38	ACTGATAGCCCTAAAACATCGCCATTTTTGAGATCCGACTACGC
Unused_m13mp18_39	GAATGGCTATTAGTCTTTAATGCGCTTTTGAGATCCGACTACGC
Unused_m13mp18_40	AGAATACGTGGCACAGACAATATTTTTTTGAGATCCGACTACGC
Unused_m13mp18_41	ATAGAACCCTTCTGACCTGAAAGCGTTTTGAGATCCGACTACGC
Unused_m13mp18_42	ATAAAAGGGACATTCTGGCCAACAGTTTTGAGATCCGACTACGC
Unused_m13mp18_43	GCAGATTCACCAGTCACACGACCAGTTTTGAGATCCGACTACGC
Unused_m13mp18_44	ATCGTCTGAAATGGATTATTTACATTTTTGAGATCCGACTACGC
Unused_m13mp18_45	ATGGAAATACCTACATTTTGACGCTTTTTGAGATCCGACTACGC
Unused_m13mp18_46	CCAGCCATTGCAACAGGAAAAACGCTTTTGAGATCCGACTACGC
Unused_m13mp18_47	CTGGTAATATCCAGAACAATATTACTTTTGAGATCCGACTACGC
Unused_m13mp18_48	GTAGAAGAACTCAAACTATCGGCCTTTTTGAGATCCGACTACGC
Unused_m13mp18_49	TGATTAGTAATAACATCACTTGCCTTTTTGAGATCCGACTACGC
Unused_m13mp18_50	AAATTAACCGTTGTAGCAATACTTCTTTTGAGATCCGACTACGC
Unused_m13mp18_51	CCGAGTAAAAGAGTCTGTCCATCACTTTTGAGATCCGACTACGC
Unused_m13mp18_52	GAAGTGTTTTTATAATCAGTGAGGCTTTTGAGATCCGACTACGC
Unused_m13mp18_53	GACAGGAACGGTACGCCAGAATCCTTTTTGAGATCCGACTACGC
Unused_m13mp18_54	AACAGGAGGCCGATTAAAGGGATTTTTTTGAGATCCGACTACGC
Unused_m13mp18_55	TCCTCGTTAGAATCAGAGCGGGAGCTTTTGAGATCCGACTACGC
Unused_m13mp18_56	GCTTTGACGAGCACGTATAACGTGCTTTTGAGATCCGACTACGC
Unused_m13mp18_57	CGCCGCTACAGGGCGCGTACTATGGTTTTGAGATCCGACTACGC
Unused_m13mp18_58	TAACCACCACACCCGCCGCGCTTAATTTTGAGATCCGACTACGC
Unused_m13mp18_59	TGGCAAGTGTAGCGGTCACGCTGCGTTTTGAGATCCGACTACGC
Unused_m13mp18_60	AAGCGAAAGGAGCGGGCGCTAGGGCTTTTGAGATCCGACTACGC
Unused_m13mp18_61	CGAACGTGGCGAGAAAGGAAGGGAATTTTGAGATCCGACTACGC
Unused_m13mp18_62	GATTTAGAGCTTGACGGGGAAAGCCTTTTGAGATCCGACTACGC

Unused_m13mp18_63	TAAATCGGAACCCTAAAGGGAGCCCTTTTGAGATCCGACTACGC
Unused_m13mp18_64	TTTTGGGGTCGAGGTGCCGTAAAGCTTTTGAGATCCGACTACGC
Unused_m13mp18_65	TACGTGAACCATCACCCAAATCAAGTTTTGAGATCCGACTACGC
Unused_m13mp18_66	AAACCGTCTATCAGGGCGATGGCCCTTTTGAGATCCGACTACGC
Unused_m13mp18_67	ACGTGGACTCCAACGTCAAAGGGCGTTTTGAGATCCGACTACGC
Unused_m13mp18_68	TTTGGAACAAGAGTCCACTATTAAATTTTGAGATCCGACTACGC
Unused_m13mp18_69	CCGAGATAGGGTTGAGTGTTGTTCCTTTTGAGATCCGACTACGC
Unused_m13mp18_70	AAATCCCTTATAAATCAAAAGAATATTTTGAGATCCGACTACGC
Unused_m13mp18_71	TGTTTGATGGTGGTTCCGAAATCGGTTTTGAGATCCGACTACGC
Unused_m13mp18_72	CTGGTTTGCCCCAGCAGGCGAAAATTTTTGAGATCCGACTACGC
Unused_m13mp18_73	TGAGAGAGTTGCAGCAAGCGGTCCATTTTGAGATCCGACTACGC
Unused_m13mp18_74	AGCTGATTGCCCTTCACCGCCTGGCTTTTGAGATCCGACTACGC
Unused_m13mp18_75	TTTCTTTTCACCAGTGAGACGGGCATTTTGAGATCCGACTACGC
Unused_m13mp18_76	GTTTGCGTATTGGGCGCCAGGGTGGTTTTGAGATCCGACTACGC
Unused_m13mp18_77	GAATCGGCCAACGCGCGGGGAGAGGTTTTGAGATCCGACTACGC
Unused_m13mp18_78	GAAACCTGTCGTGCCAGCTGCATTATTTTGAGATCCGACTACGC
Unused_m13mp18_79	TGCGCTCACTGCCCGCTTTCCAGTCTTTTGAGATCCGACTACGC
Unused_m13mp18_80	GAGTGAGCTAACTCACATTAATTGCTTTTGAGATCCGACTACGC
Unused_m13mp18_81	TAAAGTGTAAAGCCTGGGGTGCCTATTTTGAGATCCGACTACGC
Unused_m13mp18_82	TTCCACACAACATACGAGCCGGAAGTTTTGAGATCCGACTACGC
Unused_m13mp18_83	CTGTGTGAAATTGTTATCCGCTCACTTTTGAGATCCGACTACGC
Unused_m13mp18_84	ATTCGTAATCATGGTCATAGCTGTTTTTTGAGATCCGACTACGC
Unused_m13mp18_85	TAGAGGATCCCCGGGTACCGAGCTCTTTTGAGATCCGACTACGC
Unused_m13mp18_86	CAAGCTTGCATGCCTGCAGGTCGACTTTTGAGATCCGACTACGC
Unused_m13mp18_87	ACGACGTTGTAAAACGACGGCCAGTTTTTGAGATCCGACTACGC
Unused_m13mp18_88	TTGGGTAACGCCAGGGTTTTCCCAGTTTTGAGATCCGACTACGC
Unused_m13mp18_89	AGGGGGATGTGCTGCAAGGCGATTATTTTGAGATCCGACTACGC
Unused_m13mp18_90	CTCTTCGCTATTACGCCAGCTGGCGTTTTGAGATCCGACTACGC
Unused_m13mp18_91	CTGTTGGGAAGGGCGATCGGTGCGGTTTTGAGATCCGACTACGC
Unused_m13mp18_92	GCGCCATTCGCCATTCAGGCTGCGCTTTTGAGATCCGACTACGC
Unused_m13mp18_93	CGCTTCTGGTGCCGGAAACCAGGCATTTTGAGATCCGACTACGC
Unused_m13mp18_94	ATCGCACTCCAGCCAGCTTTCCGGCTTTTGAGATCCGACTACGC
Unused_m13mp18_95	GACGACGACAGTATCGGCCTCAGGATTTTGAGATCCGACTACGC
Unused_m13mp18_96	GTAACCGTGCATCTGCCAGTTTGAGTTTTGAGATCCGACTACGC
Unused_m13mp18_97	GGTCACGTTGGTGTAGATGGGCGCATTTTGAGATCCGACTACGC
Unused_m13mp18_98	AAACGGCGGATTGACCGTAATGGGATTTTGAGATCCGACTACGC

```
Unused_m13mp18_99          ACAACCCGTCGGATTCTCCGTGGGATTTTGAGATCCGACTACGC
Unused_m13mp18_100         TTCATCAACATTAAATGTGAGCGAGTTTTGAGATCCGACTACGC
```

Appendix 15: FLIP seed staple sequences

stp_80_1	TGT CAC GGT TCA GCC CTC TAC CGC CAC CCT CAG ATC GTT TAC CTG TGC TGG AGA TCC GAC TAC GC
stp_80_2	GAT GCG GTT TCA GAC GAC TTA ATA AAA CGA ACT ATT AAT CAT CCG TGA CAG AGA TCC GAC TAC GC
stp_80_3	CAG CAC AGT TCT TTC GAG TGG GAT TTT GCT AAA CTC CAC AGA CTC GGT GTG AGA TCC GAC TAC GC
stp_80_4	ACA CCG AGT TCC ATT AAA CAT AAC CGA TAT ATT CTC AGC TTG CCT TGT CCG AGA TCC GAC TAC GC
stp_80_5	GGA CAA GGT TGA ACC GAA CTA AAA CAC TCA TCT TGG AAG TTT GCC AGA CAG AGA TCC GAC TAC GC
stp_80_6	TGT CTG GCT TTG TGA ATT TCA TCA AGA GTA ATC TTC ATA AGG ACC GCA TCG AGA TCC GAC TAC GC
stp_48_1	GCA ACT CGT TTA CAA ACT CCG CCA CCC TCA GAG CGA GGC ATA GGT GCA GCG AGA TCC GAC TAC GC
stp_48_2	GTG GAC GGT TGT AAG AGC ACA GGT AGA AAG ATT CTA AAT TGG CGA GTT GCG AGA TCC GAC TAC GC
stp_48_3	GCT GCA CCT TGG AGC CTT AGC GGA GTG AGA ATA GGT CAC CAG GTC GAG CCG AGA TCC GAC TAC GC
stp_48_4	GGC TCG ACT TTG AGG ACT AGG GAG TTA AAG GCC GCT CCA AAA GCT GAC ACG AGA TCC GAC TAC GC
stp_48_5	GTG TCA GCT TCC GGA ACG TAC CAA GCG CGA AAC AAG AGG CTT GCG AAC ACG AGA TCC GAC TAC GC
stp_48_6	GTG TTC GCT TGC TTG AGA TTC ATT ACC CAA ATC ATT ACT TAG CCG TCC ACG AGA TCC GAC TAC GC
stp_95_1	GCA CCG CTT TAG GTT TAG ATA GTT AGC GTA ACG AAA ATG AAT CTG CCA ACG AGA TCC GAC TAC GC
stp_95_2	GTC ATG GCT TAA TCT ACG GAT AAA AAC CAA AAT ATA CTC AGG AGC GGT GCG AGA TCC GAC TAC GC
stp_95_3	GTT GGC AGT TTT TCT GTA GTG AAT TTC TTA AAC AAC AAC CAT GCT CAG ACG AGA TCC GAC TAC GC
stp_95_4	GTC TGA GCT TCG CCC ACG CGG GTA AAA TAC GTA AGA GGC AAA GTG CTG TCG AGA TCC GAC TAC GC
stp_95_5	GAC AGC ACT TAG AAT ACA CTG ACC AAC TTT GAA AAT AGG CTG CTG CAT CCG AGA TCC GAC TAC GC
stp_95_6	GGA TGC AGT TGC TGA CCT ACC TTA TGC GAT TTT AGG AAG AAA GCC ATG ACG AGA TCC GAC TAC GC
stp_159_1	GAT GGA CTT TGA TAA GTG GGG GTC AGT GCC TTG ACA GTC TCT AGC GTC CTG AGA TCC GAC TAC GC
stp_159_2	GGC AAC CGT TAA TTA ACT TTC CAG AGC CTA ATT TAC CAG GCG AGT CCA TCG AGA TCC GAC TAC GC
stp_159_3	AGG ACG CTT TGA ATT TAC CCC TCA GAG CCA CCA CTC TTT TCA CGG AGG CAG AGA TCC GAC TAC GC
stp_159_4	TGC CTC CGT TTA ATC AAA TAG CAA GGC CGG AAA CTA AAG GTG CGA GCA CAG AGA TCC GAC TAC GC
stp_159_5	TGT GCT CGT TAA TTA TCA TAA AAG AAA CGC AAA GAA GAA CTG CTG GTG CCG AGA TCC GAC TAC GC
stp_159_6	GGC ACC AGT TGC ATG ATT TGA GTT AAG CCC AAT AGA CGG GAG CGG TTG CCG AGA TCC GAC TAC GC
stp_208_1	GGA CCG TGT TTT CGG AAC CTG AGA CTC CTC AAG ATC CCA ATC CGA GCC ACG AGA TCC GAC TAC GC
stp_208_2	TGT GTC CGT TCA AAT AAG ATA GCA GCC TTT ACA GTA TCT TAC CAC GGT CCG AGA TCC GAC TAC GC

stp_208_3	GTG GCT CGT TAG CAT TGA TGA TAT TCA CAA ACA ACT GCC TAT GAG CGA TGG AGA TCC GAC TAC GC
stp_208_4	CAT CGC TCT TGC GAC AGA CGT TTT CAT CGG CAT TCC GCC GCC GTC ACC TGG AGA TCC GAC TAC GC
stp_208_5	CAG GTG ACT TAT TCA TAT TTC AAC CGA TTG AGG GAA TCA GTA CCT GTT GCG AGA TCC GAC TAC GC
stp_208_6	GCA ACA GGT TCG AAG CCC AGT TAC CAG AAG GAA AAA TAG AAA CGG ACA CAG AGA TCC GAC TAC GC
stp_144_1	AGG AGC ACT TGT TTT AAC CCG TCG AGA GGG TTG AAC GCT AAC CAC GGC TGG AGA TCC GAC TAC GC
stp_144_2	GGT TCG CTT TGA GCG TCT GAA CAC CCT GAA CAA AGA TAA CCC GTG CTC CTG AGA TCC GAC TAC GC
stp_144_3	CAG CCG TGT TAA CCG CCA CGT TCC AGT AAG CGT CGG TAA TAA GCC ATC ACG AGA TCC GAC TAC GC
stp_144_4	GTG ATG GCT TAT TAC CAT ATC ACC GGA ACC AGA GAC CCT CAG GCA CTC CAG AGA TCC GAC TAC GC
stp_144_5	TGG AGT GCT TGC AAC ATA CCG TCA CCG ACT TGA GGT AGC ACC GTT TGG ACG AGA TCC GAC TAC GC
stp_144_6	GTC CAA ACT TAC AAG AAT AAG ACT CCT TAT TAC GTA AAG GTG AGC GAA CCG AGA TCC GAC TAC GC
stp_31_1	CAG CTC ACT TTC ATT TTC CGT AAC ACT GAG TTT CAA AGG AAC GTC CGT CCG AGA TCC GAC TAC GC
stp_31_2	GTC AAC GCT TAG ATT TAG CGC CAA AAG GAA TTA CCA CCA CCC GTG AGC TGG AGA TCC GAC TAC GC
stp_31_3	GGA CGG ACT TAA CTA AAG ATC TCC AAA AAA AAG GCT TTT GCG GTG GAC ACG AGA TCC GAC TAC GC
stp_31_4	GTG TCC ACT TGG ATC GTC GGG TAG CAA CGG CTA CAA GTA CAA GGT GCC ACG AGA TCC GAC TAC GC
stp_31_5	GTG GCA CCT TCG GAG ATT CGC GAC CTG CTC CAT GAC GTA ACA GGC AAT GCG AGA TCC GAC TAC GC
stp_31_6	GCA TTG CCT TAA GCT GCT ACA CCA GAA CGA GTA GAT CAG TTG GCG TTG ACG AGA TCC GAC TAC GC
stp_176_1	GAT GGT CCT TGC CCG TAT CGG GGT TTT GCT CAG TGC CAG TTA CGC TGT TCG AGA TCC GAC TAC GC
stp_176_2	GCT CCT GCT TCA AAA TAA ACA GGG AAG CGC ATT AAT AAG AGC GGA CCA TCG AGA TCC GAC TAC GC
stp_176_3	GAA CAG CGT TCC GCC ACC GCC AGA ATG GAA AGC GGT AAC AGT TGC CTA GCG AGA TCC GAC TAC GC
stp_176_4	GCT AGG CAT TTG AAA CCA TTA TTA GCG TTT GCC ACC TCA GAG TGG CTC ACG AGA TCC GAC TAC GC
stp_176_5	GTG AGC CAT TGA ATA AGT GAC GGA AAT TAT TCA TGT CAC CAA CGG TCG CAG AGA TCC GAC TAC GC
stp_176_6	TGC GAC CGT TAA GAA ACA ATA ACG GAA TAC CCA AAC ACC ACG GCA GGA GCG AGA TCC GAC TAC GC
stp_63_1	CAG CCG AGT TCC TCA GAA ACA ACG CCT GTA GCA TAA CTT TCA CCA CAC CTG AGA TCC GAC TAC GC
stp_63_2	AGG ACT GCT TAC ATT ATT AAC ACT ATC ATA ACC CAC CGC CAC CTC GGC TGG AGA TCC GAC TAC GC
stp_63_3	AGG TGT GGT TAC AGT TTC TAA TTG TAT CGG TTT AGG TCG CTG GCG ACA TGG AGA TCC GAC TAC GC
stp_63_4	CAT GTC GCT TAG GCT TGC AAA GAC TTT TTC ATG ATG ACC CCC GAA CGA TGG AGA TCC GAC TAC GC
stp_63_5	CAT CGT TCT TAG CGA TTA AGG CGC AGA CGG TCA ATG ACA AGA GCC TCA CAG AGA TCC GAC TAC GC

stp_63_6	TGT GAG GCT TAC CGG ATA TGG TTT AAT TTC AAC TAC GGA ACA GCA GTC CTG AGA TCC GAC TAC GC
stp_191_1	GCA AGC GGT TAG GAT TAG AAA CAG TTA ATG CCC CAT AAA TCC TGC CTT ACG AGA TCC GAC TAC GC
stp_191_2	GAA GGT CGT TAC ATA AAA ACA GCC ATA TTA TTT AGA AGG ATT CCG CTT GCG AGA TCC GAC TAC GC
stp_191_3	GTA AGG CAT TTC ATT AAA AGA ACC ACC ACC AGA GTT CGG TCA CGC TCA TCG AGA TCC GAC TAC GC
stp_191_4	GAT GAG CGT TTA GCC CCC TCG ATA GCA GCA CCG TAG GGA AGG CGA CAC CAG AGA TCC GAC TAC GC
stp_191_5	TGG TGT CGT TTA AAT ATT TTA TTT TGT CAC AAT CCC GAG GAA CCA GTG CGG AGA TCC GAC TAC GC
stp_191_6	CGC ACT GGT TAC GCA ATA ATG AAA TAG CAA TAG CAG AGA ATA CGA CCT TCG AGA TCC GAC TAC GC
stp_mid_complex_1_1	GGC AGA CGT TCT TTT GCA ATC CTG AAT CTT ACC ATA TAA GTA CGG TCA GCG AGA TCC GAC TAC GC
stp_mid_complex_1_2	GCT GAC CGT TTA GCC CGG AAT AGG TGT ATC ACC GGC GAG AGG CGT CTG CCG AGA TCC GAC TAC GC
stp_mid_complex_2_1	CAG GTG GAT TGT AAT TGA ACC AGT CAG GAC GTT GAG AAC TGG CGT CGG TCG AGA TCC GAC TAC GC
stp_mid_complex_2_2	GAC CGA CGT TCT CAT TAT GCG CTA ATA TCA GAG AGT CAG AGG TCC ACC TGG AGA TCC GAC TAC GC
stp_mid_complex_3_1	GGA TGC CAT TCT TTT GAT CTT TCC AGA CGT TAG TTC TAA AGT CGT CCA GCG AGA TCC GAC TAC GC
stp_mid_complex_3_2	GCT GGA CGT TTT TGT CGT GAT ACA GGA GTG TAC TAT ACA TGG TGG CAT CCG AGA TCC GAC TAC GC
stp_mid_complex_4_1	CAG GAC ACT TGG AAC CGC TGC GCC GAC AAT GAC AGC TTG ATA CGG AGT ACG AGA TCC GAC TAC GC
stp_mid_complex_4_2	GTA CTC CGT TCC GAT AGT CTC CCT CAG AGC CGC CCC ACC ACC GTG TCC TGG AGA TCC GAC TAC GC
stp_mid_complex_5_1	GCC TGC GGT TTA GCA AAC TGT ACA GAC CAG GCG CGA GGA CAG AGT GCA ACG AGA TCC GAC TAC GC
stp_mid_complex_5_2	GTT GCA CTT TAT GAA CGG GTA GAA AAT ACA TAC ACA GTA TGT CCG CAG GCG AGA TCC GAC TAC GC
stp_mid_complex_6_1	GCC TGA CGT TGA ATT AGA CCA ACC TAA AAC GAA ATG CCA CTA CCG TAA GCG AGA TCC GAC TAC GC
stp_mid_complex_6_2	GCT TAC GGT TCG AAG GCA GCC AGC AAA ATC ACC ACC ATT TGG CGT CAG GCG AGA TCC GAC TAC GC

References

[1] H. Nazeran, S. Chatlapalli and R. Krishnam, "Effect of Novel Nanoscale Energy Patches on Spectral and Nonlinear Dynamic Features of Heart Rate Variability Signals in Healthy Individuals during Rest and Exercise," in *Engineering in Medicine and Biology Society, 2005. IEEE-EMBS 2005. 27th Annual International Conference of the*, Shanghai, 2005.

[2] S. Wang, C. Liu and L. Wang, "A Comparative Study of Zirconium-Based Coating on Cold Rolled Steel," *Advanced Materials Research,* Vols. 291-294, pp. 47-52, 2011.

[3] K. Pangai, C. Abraham, M. Wang, H. Nguyen, J. Coulter , T. Begley and S. Soss, "90 nm multi-level flash memory technology," in *IEEE International Symposium on Semiconductor Manufacturing*, San Jose, 2005.

[4] K. Peng, G. Cheng, B. Chen and T. Lee, "Modeling and Analysis of Micro Hard Disk Drives," in *4th International Conference on Control and Automation*, Montreal, Canada, 2003.

[5] B. Gullac and O. Akalin, "Frictional Characteristics of IF-WS2 Nanoparticles in Simulated Engine Conditions," *Tribology Transactions,* vol. 53, no. 6, 2010.

[6] D. Sept and J. A. McCammon, "Thermodynamics and Kinetics of Actin Filament Nucleation," *Biophysics Journal,* vol. 81, pp. 667-674, 2001.

[7] M. D. Welch and R. D. Mullins, "Cellular Control of Actin Nucleation," *Annu. Rev. Cell Dev. Biol.,* vol. 18, pp. 247-288, 2002.

[8] B. Yu , H.-C. Cheng, C. A. Brautigam, D. R. Tomchick and M. K. Rosen, "Mechanism of actin filament nucleation by the bacterial effector VopL," *Nature Structural & Molecular Biology,* vol. 18, no. 9, pp. 1068-1074, 2011.

[9] G. Letort , A. Z. Politi, H. Ennomani, M. Thery, F. Nedelec and L. Blanchoin, "Geometrical and Mechanical Properties Control Actin Filament Organization," *PLOS Computational Biology,* pp. 1-21, 2015.

[10] E. G. Allwood, J. J. Tyler, A. N. Urbanek, I. I. Smaczynska-de Rooij and K. R. Ayscough, "Elucidating Key Motifs Required for Arp2/3-Dependent and Independent Actin Nucleation by Las17/WASP," *PLoS ONE,* 2016.

[11] A. S. Coutts and N. B. L. Thangue, "Regulation of actin nucleation and autophagosome formation," *Cellular and Molecular Life Sciences,* pp. 3249-3263, 2016.

[12] M. Moritz, M. B. Braunfeld, V. Guenebaut, J. Heuser and D. A. Agard, "Structure of the y-tubulin ring complex: a template for microtubule nucleation," *Nature Cell Biology,* vol. 2, pp. 365-370, 2000.

[13] E. A. Fishel and R. Dixit, "Role of nucleation in cortical microtubule array organization: variations on a theme," *The Plant Journal,* vol. 75, pp. 270-277, 2013.

[14] J. M. Kollman, C. H. Greenberg, S. Li, M. Moritz, A. Zelter, K. K. Fong, J.-J. Fernandez, A. Sali, J. Kilmartin, T. N. Davis and D. A. Agard, "Ring closure activates yeast yTuRC for species-specific microtubule nucleation".

[15] S. Petry and R. D. Vale, "Microtubule nucleation at the centrosome and beyond," *Nature Cell Biology,* vol. 17, no. 9, pp. 1089-1093, 2015.

[16] M. Wieczorek, S. Bechstedt, S. Chaaban and G. J. Brouhard, "Microtubule-associated proteins control the kinetics of microtubule nucleation," *Nature Cell Biology,* vol. 17, no. 7, pp. 907-916, 2015.

[17] K. Masoud, E. Herzog, M.-E. Chaboute and A.-C. Schmit, "Microtubule nucleation and establishement of the mitotic spindle in vascular plant cells," *The Plant Journal,* vol. 75, pp. 245-257, 2013.

[18] J. Sharma, R. Chhabra, Y. Liu, Y. Ke and H. Yan, "DNA-templated self-assembly of two-dimensional and periodical gold nanoparticle arrays," *Angew. Chem. Int. Ed.,* vol. 45, pp. 730-735, 2006.

[19] J. D. Carter and T. H. Labean, "Organization of inorganic nanomaterials via programmable DNA self-assembly and peptide molecular recognition," *ACS Nano,* vol. 5, pp. 2200-2205, 2011.

[20] Y. Y. Pinto, J. D. Le, N. C. Seeman, K. Musier-Forsyth, T. A. Taton and R. A. Kiehl, "Sequence-encoded self-assembly of multiple-nanocomponent arrays by 2D DNA scaffolding," *Nano Letters,* vol. 5, pp. 2399-2402, 2005.

[21] P. W. K. Rothemund, "Folding DNA to create nanoscale shapes and patterns," *Nature,* vol. 440, pp. 297-302, 2006.

[22] A. Rajendran, M. Endo, Y. Katsuda, K. Hidaka and H. Sugiyama, "Programmed two-dimensional self-assembly of multiple DNA origami jigsaw pieces," *ACS Nano,* vol. 5, pp. 665-671, 2010.

[23] P. K. Lo, P. Karam, F. A. Aldaye, C. K. McLaughlin, G. D. Hamblin, G. Cosa and H. F. Sleiman, "Loading and selective release of cargo in DNA nanotubes with longitudinal variation," *Nat. Chem.,* vol. 2, pp. 319-328, 2010.

[24] C. M. Erben, R. P. Goodman and A. J. Turberfield, "Single-molecule protein encapsulation in a rigid DNA cage," *Angew. Chem. Int. Ed. Engl.,* vol. 45, pp. 7414-7417, 2006.

[25] B. Yurke, A. J. Turberfield, A. P. Mills Jr., F. C. Simmel and J. L. Neumann, "A DNA-fuelled molecular machine made of DNA," *Nature,* vol. 406, pp. 605-608, 2000.

[26] J.-S. Shin and N. A. Pierce, "A synthetic DNA walker for molecular transport," *J. Am. Chem. Soc.,* vol. 126, pp. 10834-10835, 2004.

[27] Y. Tian, Y. He., Y. Chen, P. Yin and C. Mao, "A DNAzyme that walks processively and autonomously along a one-dimensional track," *Angew. Chem. Int. Ed. ,* vol. 44, pp. 4355-4358, 2005.

[28] S. F. J. Wickham, M. Endo, Y. Katsuda, K. Hidaka, J. Bath, H. Sugiyama and A. J. Turberfield, "Direct observation of stepwise movement of a synthetic molecular transporter," *Nat. Nano,* vol. 6, pp. 166-169, 2011.

[29] T.-J. Fu and N. C. Seeman, "DNA Double-Crossover Molecules," *Biochemistry,* vol. 32, no. 13, pp. 3211-3220, 1993.

[30] E. Winfree, F. Liu, L. A. Wenzler and N. C. Seeman, "Design and self-assembly of two-dimensional DNA crystals," *Nature,* vol. 394, pp. 539-544, 1998.

[31] A. M. Mohammed and R. Schulman, "Directing Self-Assembly of DNA Nanotubes Using Programmable Seeds," *Nano letters,* pp. 4006-4013, 2013.

[32] R. J. Davey and J. Garside, From Molecules to Crystallizers, Oxford University Press, 2010.

[33] D. K. Agrawal, S. Reinhart, A. M. Mohammed, T. D. Jorgenson and R. Schulman, "Terminating DNA Tile Assembly with Nanostructured Caps".

[34] V. A. Bloomfield, D. M. Crothers and I. Tinoco, Jr., Nucleic Acids: Structures, Properties, and Functions, University Science Books, 1999.

[35] C. E. Castro, F. Kilchherr, D.-N. Kim, E. L. Shiao, T. Wauer, P. Wortmann, M. Bathe and H. Dietz, "A primer to scaffolded DNA origami," *Nature Methods,* vol. 8, no. 3, pp. 221-229, 2011.

Seth Reinhart

1233 Chestnut Street
Pottstown, PA 19464
610-487-5300 | sreinha7@gmail.com

EDUCATION

Johns Hopkins University **Baltimore, MD**
Master of Science in Chemical and Biomolecular Engineering Expected May 2017
Johns Hopkins University **Baltimore, MD**
Bachelor of Science in Chemical and Biomolecular Engineering (GPA: 3.22) May 2016

WORK & LEADERSHIP EXPERIENCE

Department of Chemical and Biomolecular Engineering **Baltimore, MD**
Research Assistant, Schulman Lab September 2014 – Present

- Researching nucleation and self-assembly of DNA nanotube structures
  - Designed and built novel caps to selectively control the length of DNA nanotube structures
    - Performed key experiments using fluorescence microscopy to reveal characteristics of these caps
    - Analyzed and quantified data to characterize caps
  - Characterizing DNA nanotube nucleation to target areas of improvement
    - Currently identifying these improvement areas
    - Designing novel structures in line with these improvement areas using Autodesk Maya

Teaching Assistant for Current Topics in DNA Technology Practicum

- Instructing undergraduate students in lab techniques necessary for studies on DNA nanotube structures
- Lecturing students on recent developments in the field of DNA nanotechnology

Related Awards

- Graduate Student & Postdoctoral Fellow Research & Education Award (2017)

Reinhart Painting & Paperhanging **Pottstown, PA**
Summer Crew Leader Summers of 2013 and 2014

- Led a team to complete projects in a timely manner resulting in increased profits for the company
- Communicated with clients about project goals
- Handled day-to-day management of assigned projects

Thread: The New Social Fabric **Baltimore, MD**
Grandparent (Team Director) November 2012 – May 2016

- As grandparent, directed 5 teams with approximately 30 members
- Mentored underserved students starting in their freshmen year of high school
- Recruited between 10-20 volunteers to the club
- Organized and participated in events for the mentors and their students

PUBLICATIONS

Agrawal, D., Mohammed, A., **Reinhart, S.**, Jorgenson, T., Schulman, R. Dynamic control of DNA tile nanotube nucleation and elongation. *21st International Conference on DNA Computing and Molecular Programming. Wyss Institute for Biologically Inspired Engineering, Harvard University. 2015.*

Seth Reinhart

1233 Chestnut Street
Pottstown, PA 19464
610-487-5300 | sreinha7@gmail.com

Agrawal, D., **Reinhart, S.**, Mohammed, A., Jorgenson, T., Schulman, R. Terminating DNA Tile Assembly with Nanostructured Caps. *Submitted.*

SKILLS & INTERESTS

Computer Skills: MATLAB, Autodesk Maya, Cadnano
Interests: Reading, Learning German, American History, Running, and Film